Tutor/s

Dr. E. Carolina Sañudo
Departament de Química Inorgànica i Orgànica

Dr. Arántzazu González Campo
ICMAB-CSIC

Grau de Química

Treball Final de Grau

Synthesis of Biocompatible Metal-Organic Frameworks and their immobilization on surfaces

Síntesi de Metal-Organic Frameworks Biocompatibles i la seva immobilització en superfícies

Andrea Suárez Herrera

June 2021

Universitat de Barcelona

B:KC Barcelona Knowledge Campus
Campus d'Excel·lència Internacional

A la meva família i amics, per estar sempre al meu costat.

A Aurora, pel seu suport incondicional.

A Arancha, Daniel i Raquel, per ajudar-me en tot el que he necessitat.

Als meus amics de la carrera, que han fet d'aquesta experiència una memòria inoblidable.

REPORT

CONTENTS

1. SUMMARY

Metal-Organic Frameworks (MOFs) are porous materials composed of metal ions or clusters linked to organic ligands by coordination bonds, leading to the formation of structures with two or more dimensions built from repeatable units. The biological application of MOFs has been studied over the past few decades, leading to the synthesis of Biological MOFs (Bio-MOFs). These biologic compatible structures are mainly employed for the delivery of active ingredients and for therapeutic and diagnostic applications. On the other hand, the integration of MOFs in devices has involved the necessity to prepare films of MOFs and their growth on functionalized surfaces, in order to obtain surface-coordinated metal-organic frameworks (SURMOFs). Therefore, in this work the preparation of the $[Zn_3(CCM)_2]$ Bio-MOF based on Zn(II) and curcumin (CCM), and its corresponding SURMOF have been studied. First, two different methodologies were developed for its synthesis: solvothermal and microwave-assisted synthesis. Consequently, the obtained products were analysed via X-ray Photoelectron Spectroscopy and Scanning Electron Microscopy, in order to corroborate the formation and crystallinity of the Bio-MOF. On the other hand, the preparation of the corresponding $[Zn_3(CCM)_2]$ SURMOF has also been studied using two different monolayers as nucleation points: curcumin SAM and eugenol derivative SAM. For the curcumin SAMs, the localized attachment of curcumin on the surfaces was carried out by the reaction of the curcumin with terminal imidazole monolayer. For the eugenol-based SAM, first a derivative of the eugenol with reactive $–Si(OEt)_3$ groups was synthesized. Both strategies lead to the formation of patterned curcumin monolayers, obtained via micro-contact printing. Finally, the growth of the of the $[Zn_3(CCM)_2]$ SURMOF on the active monolayers was performed via drop casting, layer-by-layer and solvothermal methodologies, optimizing parameters such as solvents, times and blocking of the non-patterned areas. The surfaces were characterized using fluorescence microscopy, contact angle measurements, X-ray Photoelectron Spectroscopy, Scanning Electron Microscopy and Energy-dispersive X-ray spectroscopy.

Keywords: Metal-Organic Frameworks (MOFs), Biological Metal-Organic Frameworks (Bio-MOFs), Self-Assembled Monolayers (SAMs), Surface-coordinated Metal-Organic Frameworks (SURMOFs), curcumin (CCM), triethoxysilane, eugenol, micro-contact printing (μCP).

2. RESUM

Els Metal-Organic Frameworks (MOFs) són materials porosos compostos per ions metàl·lics enllaçats a lligands orgànics a través d'enllaços de coordinació, donant lloc a la formació d'estructures amb dues o més dimensions construïdes a partir d'unitats repetibles. L'aplicació biològica dels MOFs ha estat estudiada en les últimes dècades, donant lloc a la síntesi de MOFs biològics (Bio-MOFs). Aquestes estructures biològicament compatibles s'utilitzen principalment pel lliurament d'ingredients actius i per aplicacions terapèutiques i diagnòstiques. D'altra banda, la integració dels MOFs en dispositius ha implicat la necessitat de preparar pel·lícules de MOFs i el seu creixement en superfícies funcionalitzades, per tal d'obtenir metal-organic frameworks coordinats a superfícies (SURMOFs). Per tant, en aquest treball la preparació del Bio-MOF $[Zn_3(CCM)_2]$ compost per Zn(II) i curcumina (CCM) i el seu corresponent SURMOF han estat estudiats. En primer lloc, es van desenvolupar dues metodologies diferents per la seva síntesi: solvotermal i síntesi promoguda per microones. En conseqüència, els productes obtinguts van ser analitzats per Espectroscòpia Fotoelectrònica de Raigs X i per Microscòpia Electrònica d'Escombratge, per tal de corroborar la formació i la cristal·linitat del Bio-MOF. D'altra banda, la preparació del corresponent $[Zn_3(CCM)_2]$ SURMOF ha estat també estudiada utilitzant dues monocapes diferents com a punts de nucleació: la SAM de curcumina i la SAM derivada d'eugenol. Per les SAMs de curcumina, la unió localitzada de la curcumina a les superfícies es va dur a terme per la reacció de la curcumina amb els grups imidazole terminals de la monocapa. Per la SAM basada en l'eugenol, primer es va sintetitzar un derivat de l'eugenol amb grups reactius $-Si(OEt)_3$. Ambdues estratègies condueixen a la formació de monocapes de curcumina amb patrons, obtingudes mitjançant micro-contact printing (μCP). Finalment, el creixement del SURMOF $[Zn_3(CCM)_2]$ sobre les monocapes actives es va realitzar a través de metodologies com drop casting, layer-by-layer i solvotermal, optimitzant paràmetres com dissolvents, temps i bloqueig de les àrees sense patró. Les superfícies es van caracteritzar utilitzant microscòpia de fluorescència, mesures d'angle de contacte, Espectroscòpia Fotoelectrònica de Raigs X, Microscòpia Electrònica d'Escombratge i Espectroscòpia de Raigs X dispersiva.

Paraules clau: Metal-Organic Frameworks (MOFs), Metal-Organic Frameworks Biològics (Bio-MOFs), Monocapes Autoassemblades (SAMs), Metal-Organic Frameworks coordinats a superficies (SURMOFs), curcumina (CCM), trietoxisilà, eugenol, micro-contact printing (μCP).

3. INTRODUCTION

Materials with at least one dimension in the nano scale are referred as nanomaterials. These compounds can be distinguished from bulk materials by exhibiting distinctive properties due to their small size. Lately, materials built from nanocomposites have emerged as promising candidates for a wide range of applications, including catalysis and sensing.[1,2] Over the past few decades, Metal-Organic Frameworks (MOFs) have attracted a lot of research interest due to their unique structures, promising capabilities, and chemical and physical properties.[3]

3.1. METAL-ORGANIC FRAMEWORKS (MOFS)

MOFs are synthetic materials composed of metal ions or clusters linked to organic ligands by coordination bonds. These components assemble into two-dimensional or three-dimensional network structures built from repeatable units, leading to the formation of crystalline structures with cavities with different shapes and sizes.[4,5]

In 1999, the first MOF was reported by Williams et al., which received the name of HKUST-1 and was composed of Cu(II) clusters coordinated to benzene tricarboxylate ligands. Shortly after, Yaghi et al. reported a MOF called MOF-5, composed of Zn(II) clusters linked to benzene dicarboxylate ligands and characterized for being extremely porous (Figure 1).[6]

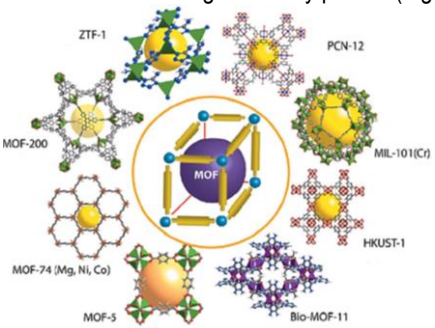

Figure 1. Representation of reported MOFs (extracted image from Yang Zhao et al. *Energy Storage Mat.* **2016**, *2*, 35-62).

MOFs are characterized for having a modular crystalline structure, which provides the opportunity of obtaining a wide range of structures with specific properties, topology and functionality.[3] Regarding to the components of a MOF, lanthanides, alkaline metals, and transition metals are used as metal ions and carboxylates, phosphonates and azolates as organic ligands, among many others.[4] Depending on the functionality and the length of the organic linkers, pore size and shape of MOFs can vary alongside with density and surface area.[3]

These materials are characterized for their thermal stability and flexible tailorability[7], but the main features that make MOFs distinctive from other porous materials are their high porosity (50% of the total volume or even more) and large surface area (up to 10.000 m^2/g for some reported MOFs).[8]

The control of the structure, porosity and functionality of MOFs gave rise to numerous applications, such as gas storage, catalysis, molecular recognition, chemical sensing, drug carriers and biomedical applications.[9,10] In addition, MOFs have great absorption capacity, which is significantly influenced by the size and shape of the structure.[11]

Regarding the MOFs synthesis, different approaches have been reported such as microwave-assisted, conventional heating, solvothermal, sonochemical, electrochemical, mechanochemical and dry-gel conversion, which are the most common techniques to obtain MOFs.[12,13]

3.2. Biological Metal-Organic Frameworks (Bio-MOFs)

Recently, MOFs have also been studied for biological applications, giving rise to the synthesis of Bio-MOFs. These structures can be understood under two different definitions: Bio-MOFs are porous MOFs that can be used in a wide range of applications related to biology and medicine or structures that are composed of at least one organic ligand that is a biomolecule.[9]

The main requirement for bioapplications is biocompatibility, and the interaction between the material and the living organism is the reason that defines it. Therefore, the potential toxicity of MOFs needs to be considered. It is reported that morphology, surface charge and size influence the function of MOFs, meaning that an unsuitable formulation can generate serious toxic issues and lower efficacies.[4] Hence, the properties of these structures must be consistent when entering a living entity.[13]

Regarding chemical composition, it is compulsory to consider the toxicity of the framework components (organic ligands, metal ions, solvents and counterions) besides de toxicity of the MOF. Therefore, the elements of a Bio-MOF must be carefully selected, so stability, particle size, efficacy, surface properties, morphology and toxicology can be under control.[9]

To control the toxicity factor, Bio-MOFs employ non-toxic endogenous cations, such as Ca^{2+}, Mg^{2+}, $Fe^{2+/3+}$ and Zn^{2+} and, as for organic ligands, biomolecules are used, including amino acids, porphyrins, cyclodextrins, proteins, nucleobases, carbohydrates, and biological carboxylic acids, among many others. In addition, amorphous MOFs can be synthesized due to the flexibility of the biomolecules.[11] Furthermore, the solvent utilized is another factor to take into consideration and the usage of non-toxic solvents enables the achievement of more structures that are biologically compatible.[13]

3.3. CURCUMIN BIO-MOF ($[Zn_3(CCM)_2]$)

For the synthesis of Bio-MOFs, it is preferable to use symmetric molecules because it has been proven that the symmetry of the organic ligand is a key factor to produce highly porous Bio-MOFs. Nevertheless, most biomolecules are not characterized for having symmetry. One of the biomolecules that present symmetry is curcumin (CCM)[11]. CCM is a natural antioxidant extracted from the rhizome of the turmeric plant and is known for its wide range of applications such as cancer treatment, antivirus, anticoagulant blood, antibacterial, anti-HIV and many more.[14,15] However, free CCM tends to be sensitive to light, high temperatures, alkaline or neutral conditions, degrades easily and has low solubility in water.[16]

CCM structure is characterized for having -OH, $-OCH_3$ and β-diketone groups as coordination sites (Figure 2a), resulting in an obtention of an extensive variety of structures upon coordination with metal ions.[11] In addition, CCM is a fluorescent molecule, meaning that it is suitable for fluorescence probing and sensing applications.[17]

A structural feature of CCM is its tautomerism (Figure 2b). The keto-enol tautomer is the predominant in organic solvents, especially in polar protic and aprotic solvents, and aqueous solutions. The keto tautomer is formed in apolar solvents, but the equilibrium is not fully displaced, and the main tautomer is not defined.[18] Moreover, studies have demonstrated that both double bonds present in the compound have trans (E) configuration.[19]

Using CCM as organic ligand and Zn(II) as coordination metal has led to the formation of a Bio-MOF called Medi-MOF-1 ($[Zn_3(CCM)_2]$)[15]. This stable porous framework is characterized for having high surface area (3002 m^2/g) and serves as a host framework for the delivery of molecules such as ibuprofen[20].

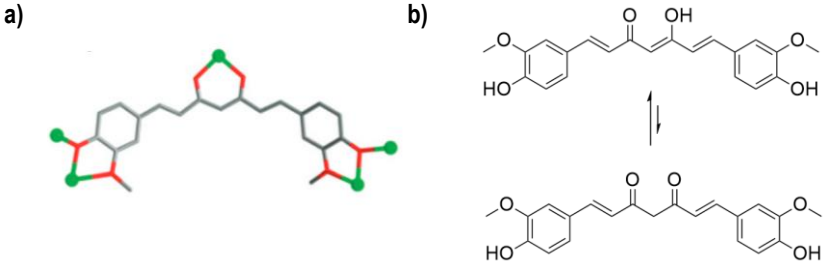

Figure 2. Curcumin a) coordination sites (extracted image from Hongmin Su et al, ref 20) and b) tautomerism.

The size of a Bio-MOF is a key factor for its synthesis and biocompatibility. However, the control over the size remains difficult. A possibility for medi-MOF-1's size reduction has been developed by Xiaodong Feng et al. using capping ligands such as Eugenol (EU).[15]

3.4. SURFACE-COORDINATED METAL-ORGANIC FRAMEWORKS (SURMOFS)

Nowadays, having precise control over MOFs during their application has gained attention. The presence of a solid substrate where the MOF can attach to opens possibilities not accessible for the typical MOFs powders obtained by the normal bulk synthesis schemes. Consequently, MOF thin films can grow onto these substrates.

Regardless, it is necessary to distinguish between two different classes of MOF thin films: polycrystalline films and SURMOFs. Regarding polycrystalline films, these films are obtained from the assembly of MOF crystals between each other randomly oriented and deposited onto a substrate. If interactions with the corresponded substrate take place, the attachment of crystals in one specific direction is enhanced. In this particular case, the size of the crystals lies in the micrometer scale, and the thickness of the film is influenced by the size of these crystals. These films can be obtained from the Growth at Room Temperature or Slow Diffusion Reactants, among many others.

As for SURMOFs, these films are ultrathin crystal multilayers that are excellently oriented at least in one direction. These films are characterized for presenting low roughness, almost no

defects and are ideally built from large in-plane single crystals-domains. In order to have precise control over the thickness of a SURMOF, two different procedures are employed for the synthesis of SURMOFs: the Langmuir-Blodgett Layer-by-Layer Deposition method, where MOF layers are transferred onto a solid substrate by Langmuir-Blodgett instrument and rinsed between steps, and Liquid-phase epitaxy, which is based on the adsorption of the components from the solution to the surface. In addition, SURMOFs present great potential as catalysts, sensors and electronic devices.[21,22]

With the aim of controlling the size, crystallinity and orientation of the crystals, functionalized substrates with ordered molecules or self-assembled monolayers (SAMs) are used.[21,22]

SAMs are oriented two-dimensional arrangements of ordered molecules formed spontaneously onto a surface forming a layer. Nearly all biomolecules interact and self-assemble between each other forming ordered structures depending on their functionality.[23]

The structure of a SAM consists of three parts: the head group, which has affinity for the substrate and binds onto it; the aliphatic chain, which orientates and orders the layer, provides thickness to it and has a length between 1-3 nm; the terminal group, which defines the reactivity and the chemical and physical properties of the SAM (Figure 3).[24] In addition, SAMs can be categorized into two different groups: SAMs formed from small molecules such as thiols and silanes and polymer SAMs, characterized for having large chains of macromolecules.[23]

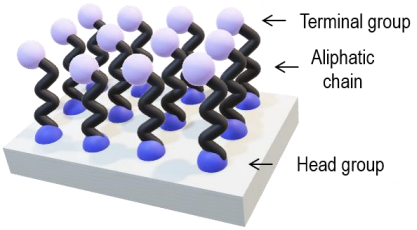

Figure 3. SAM structure representation consisting in the heard group, aliphatic chain, and terminal group.

The functionalization of surfaces allows the modification of properties, obtain new applications and, most importantly, a better management of a system when it is anchored onto a surface. The attachment between the substrate and the molecule takes place through covalent bond because techniques like physical adsorption or interactions such as electrostatic, hydrophobic or Van der Waals suffer from instability.[24]

Furthermore, SAMs have drawn attention because of their capability of tailoring surface properties such as adhesion, wetting behaviour and corrosion of silica, metal and glass surfaces. Metal substrates are altered by silanes or thiols meanwhile glass and silicon substrates are altered by alkylsilanes. Also, they are widely used as film transistors, sensors and patterning in electronic devices.[24,25]

Many applications require patterned monolayers instead of completely covered monolayers (SAMs). The pattern allows the growth of a SURMOF in specific localizations of the substrate, leading to an improvement of the orientation and selectivity of the crystals.[26] The pattern can be obtained from two different strategies: bottom-up and top-down methods.

Top-down method produces small structures based on miniaturization from bulk material whereas bottom-up method forms ordered nano- and micro-structures from smaller components. Microcontact Printing (μCP) is a bottom-up method, which belongs to the soft lithography field, and enables the obtention of micrometer or nanometer sized patterns of SAMs. Microcontact printing uses a master with features, usually a silicon wafer, and poly(dimethylsiloxane) (PDMS) to create stamps, which will be used to transfer the pattern from the master to the substrate. The microcontact printing consist in several steps (Figure 4). First, the inking of the stamp. Second, the printing step, which involves putting in contact the surfaces with the stamp. Thanks to the pattern of the stamp, just the zones with protrusions are in contact with the substrate and therefore the molecules can be transferred to the surface mostly through covalent bonds. This process allows the formation of a micro-patterned substrate, where the patterned SAM acts as a nucleation point for the SURMOFs' growth.[27,28]

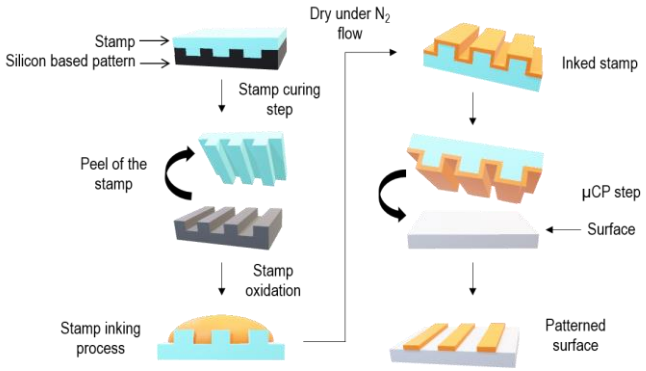

Figure 4. Microcontact Printing (μCP) process.

4. OBJECTIVES

Following the idea to prepare Bio-MOFs growth on surfaces, the main objective of this project is to obtain localized SURMOFs based on curcumin (CCM) and Zn(II) by its crystallization on active self-assembled monolayers on SiO_2 surfaces. In order to achieve the main objective, the following secondary objectives have been proposed:

1) Preparation and characterization of $[Zn_3(CCM)_2]$ Bio-MOF in solution by solvothermal and microwave-assisted synthesis techniques in order to stablish the conditions of the Bio-MOF growth.
2) Preparation and characterization of active surfaces for the growth of the curcumin-based Bio-MOFs using curcumin and eugenol-based SAMs.
3) Development of strategies for the growth of CCM-based SURMOF on patterned CCM or eugenol (EU) SAMs.
4) Characterization of the surfaces upon the SURMOF growth.

5. EXPERIMENTAL SECTION

5.1. MATERIALS, INSTRUMENTATION AND METHODS

5.1.1. Materials and instrumentation

CCM synthesis: boron oxide (B_2O_3) (99.98%), 4-hydroxy-3-methoxybenzaldehyde (99%) (vanillin), tributylborate (≥99%) and n-butylamine (99.5%) were purchased from Sigma-Aldrich. 2,4-pentanodione (99%) (acetylacetonate) was purchased from Merck KGaA. Hydrochloric acid (1%) was purchased from Labkem. Diethyl ether (pure) and ethyl acetate (pure) were purchased from Carlo Ebra.

$EuSi(OEt)_3$ synthesis: Eugenol (99%) and triethoxysilane (95%) were purchased from Sigma-Aldrich. Karstedt's catalyst (3-3.5% Pt) was purchased from abcr GmbH. Dry toluene (99.9%) was purchased from Scharlab S.L.

Stamps: Poly(dimethylsiloxane) (PDMS) and a curing agent (Sylgard 184) were purchased from Dow Corning.

SAMs preparation: N-(3-(trimethoxysilyl)propyl)ethylenediamine (97%) (TPEDA), N,N'-carbonyldiimidazole (CDI), rhodamine B isothiocyanate (RITC), 6-aminofluorescein (6-AF), isopropanol and 1-bromo-2,2-dimethylpropane (98%) were purchased from Sigma-Aldrich. Sulphuric acid (96%) (H_2SO_4), methanol (MeOH) (pure) and acetone (pure) were purchased from Carlo Ebra. Hydrogen peroxide (30%) (H_2O_2), dry tetrahydrofuran (THF) (99.9%) dry dichloromethane (DCM) (99.9%) and dry toluene (99.9%) were purchased from Scharlab S.L.

Substrates: glass slides were purchased from Menzel and silicon wafers doped with p-Boron were purchased from University Wafer P.

[$Zn_3(CCM)_2$] synthesis in solution: Zinc acetate dihydrate (≥99%) ($Zn(OAc)_2 \cdot 2H_2O$), N,N-dimethylacetamine (99.8%) (DMA) and N,N-Diethylacetamide (97%) (DEA) were purchased from Sigma-Aldrich. N,N'-Dimethylformamide (DMF) (99.9%) was purchased from Romil. Methanol (MeOH) (pure) and ethanol (EtOH) (pure) were purchased from Carlo Ebra.

Instrumentation: ^{1}H NMR spectra were collected by a Bruker Avance DPX-360Hz. FTIR-ATR spectra were collected with a JASCO 6800. Contact angle measurements were performed with an Attension from Iberlaser.

Powder X-ray diffraction spectra were obtained using a Siemens D-5000 with Kα average of Cu (1.5418 Å). Scanning electron microscopy images and EDX analysis were obtained with Quanta FEI 200 FEG-ESEM operating at low vacuum (50 Pa) with 5 kV and 3.5 spot.

UV-vis spectra in solution were obtained with a Cary 5 Spectrophotometer and UV-vis spectra of solid samples were obtained with a JASCO V-780 Spectrophotometer. Fluorescence analysis in solution and in solid were performed with Varian Fluorimeter. Optical and fluorescent microscopy images were obtained with Olympus RX51. Vacuum chamber desiccator (Vacuo-Temp) was purchased from J.P. SELECTA. XPS spectra were obtained with SPECS Phoibos 150 hemispherical energy analyzer.

5.1.2. Methods

PDMS stamps preparation: stamps were prepared by blending a 10:1 (w/w) mixture of poly(dimethylsiloxane) (PDMS) and a curing agent (Sylgard 184) against different patterned masters. In order to prevent pattern distortion, the masters containing the mixture were enclosed in low vacuum chamber desiccator to remove air bubbles trapped in the PDMS. Three cycles of evacuation and air refill were done before leaving them under vacuum for 45 minutes.

Then, the PDMS was left curing in an oven at 70 ºC overnight. After this period of time, the stamps were cooled down and peeled off from the master.

The patterns of the stamps consisted in straight lines separated by a certain distance. Four different types of patterns were used: lines of 5 µm with 10 µm separation, lines of 10 µm with 20 µm separation, lines of 100 µm with 35 µm separation and a flat stamp (stamp without features).

UV-Vis/Fluorescence spectroscopy: two different measurements were done for CCM: in solid state, CCM/KBr pellet with a final concentration of 9100 ng CCM/mg KBr for UV-Vis and the minimum quantity (mg) for fluorescence spectroscopy, and in solution, 10^{-5} M CCM in CH_2Cl_2 . As for $EUSi(OEt)_3$, measurements were done using 10^{-5} M solution in CH_2Cl_2.

5.2. SYNTHESIS

5.2.1. Curcumin synthesis (CCM)[29]

B_2O_3 (0.5 g, 7.18 mmol) was dissolved in a solution of acetylacetonate (AcAc) (1 ml, 9.78 mmol) and ethyl acetate (5 ml, 51.19 mmol) and heated and stirred at 60 ºC for 1 h. Meanwhile, a solution of vanillic aldehyde (2.95 g, 19.39 mmol), tributylborate (11 ml, 3.71 mmol) and ethyl acetate (20 ml, 204.74 mmol) was prepared and stirred for 45 minutes without temperature.

After this time, the vanillic aldehyde solution was added to the solution of AcAc and B_2O_3 and the solution was stirred and heated at 60 ºC for 1 h. The solution was cooled down to room temperature and a solution of n-butylamine (0.5 ml, 5.06 mmol) in ethyl acetate (10 ml, 102.38 mmol) was added dropwise. The reaction mixture was sealed and stirred for 48 hours without temperature.

Then, the precipitate was filtered under vacuum, washed with ethyl acetate and dried with a small amount of diethyl ether. The solid was introduced in the same previously used flask and a solution of HCl 1% (50 ml, 16.46 mmol) was added. The mixture was stirred and heated at 60 ºC for 2 h. The solid was filtered, washed with water, and dried with diethyl ether, obtaining curcumin as an orange solid (1.79 g, 50 % yield).

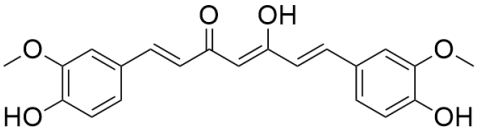

Curcumin. ^{1}H-NMR (DMSO-d_6, 360 MHz, 25 ºC, δ (ppm)): 3.83 (s, 6H), 6.05 (s, 1H), 6.76 (d, J = 16 Hz, 2H), 6.82 (d, J = 8.2 Hz, 2H), 7.15 (d, J = 8.2 Hz 2H), 7.32 (s, 2H), 7.54 (d, J = 16 Hz, 2H), 9.67 (s, 2H), 16.41 (s, 1H). FTIR-ATR: 3454, 2940, 1632, 1594, 1515, 1291, 1037, 959 cm^{-1}. UV-Vis (λ absorption, solid, nm): 421. UV-Vis (λ absorption, 10^{-5} M, CH_2Cl_2, nm): 226, 420. Fluorescence (λ emission, solid, nm): 573. Fluorescence (λ emission, 10^{-5} M, CH_2Cl_2, nm): 483, 497.

5.2.2. EUSi(OEt)$_3$ synthesis[30]

Eugenol (1.54 ml, 9.94 mmol), 5 drops of Karstedt's catalyst and dry toluene (2 ml, 18.82 mmol) were mixed in a bottom round flask under argon, stirred and heated at 40 ºC for a few minutes. Then, HSi(OEt)$_3$ (1.84 ml, 9.97 mmol) was added dropwise to the solution and the mixture was left stirring for 30 minutes at 40 ºC. The excess of HSi(OEt)$_3$ was removed under vacuum at 52 ºC, obtaining EUSi(OEt)$_3$ as a light brown oil (3.09 g, 95 %). (TLC: hexane:chloroform (8:2) and 5% of THF).

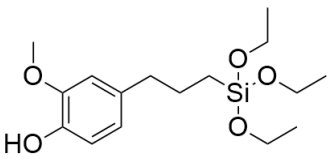

EUSi(OEt)$_3$. ^{1}H-NMR ($CDCl_3$, 360 MHz, $CDCl_3$, 25 ºC, δ (ppm)): 0.66 (t, J = 7.2 Hz, 2H), 1.21 (q, 9H), 1.71 (m, 2H), 2.57 (t, J = 7.5 Hz, 2H), 3.80 (q, 6H), 3.87 (s, 3H), 5.52 (s, 1H), 6.68 (d, J = 7.2 Hz, 2H), 6.83 (s, 1H). FTIR-ATR: 3300-3500, 2974, 2928, 1603, 1513, 1100 cm^{-1}. UV-Vis (λ absorption, 10^{-5} M, CH_2Cl_2, nm): 276. Fluorescence (λ emission, 10^{-5} M, CH_2Cl_2, nm): 320.

5.2.3. [Zn$_3$(CCM)$_2$] MOF synthesis[15,20]

Modified solvothermal and microwave-assisted methodologies were followed to synthesize the MOF in solution. Several solutions were prepared: i) CCM:Zn 1:1.78 in DMA:MeOH, DMF:MeOH, DEA:MeOH, DEA:EtOH (1:1); ii) CCM:Zn 1.78:1 in DMA:MeOH 1:1 and iii) CCM:Zn 3:2 in DMA:MeOH 1:1. For the solvothermal approach, the vials were closed and placed in the oven for 4 days at 85 ºC. On the other hand, for microwave-assisted approach, the solutions were heated at 100 ºC for different periods of time (2.5, 1.5, 3.5 and 2.5 hours, respectively; DEA experiments could not be performed via microwave-assisted approach).

5.3. SELF-ASSEMBLED MONOLAYERS PREPARATION

NH_2 SAMs: the substrates were activated in a piranha solution (H_2SO_4 and H_2O_2 3:1) for 30 minutes. Afterwards, each surface was rinsed several times with MiliQ water and dried with a nitrogen flow. Hydroxyl activated surfaces were placed inside a low vacuum chamber desiccator with 0.1 ml of TPEDA and were incubated to 70 ºC overnight. After this time, each substrate was rinsed with absolute ethanol and dry dichloromethane and dried with a nitrogen flow.

RITC control: the stamps were rinsed with MiliQ water and dry with nitrogen flow before used. The stamps were inked with a 1 mM RITC solution in MeOH with drops of the solution onto the stamp for 10 minutes. Then, the stamps were dried with a nitrogen flow, and brought into contact with the surface by applying 10 g of pressure for 10 minutes. Finally, the substrates were rinsed with MeOH and dried with a nitrogen flow.

IM SAMs: the amine-terminated substrates were incubated with saturated CDI solution in freshly distilled THF under argon atmosphere for 4 h or overnight. After this time, the substrates were rinsed with distilled THF and dried with a nitrogen flow.

6-AF control: the stamps were oxidized for 5 minutes, inked with 1 mM 6-AF solution for 10 minutes and put into contact with the IM SAMs for 10 minutes by applying 10 g of pressure. Then, the substrates were rinsed with MeOH and dried with a nitrogen flow.

Patterned CCM substrates: the stamps were inked with 1 mM CCM solution in acetone for 1 hour. Subsequently, the stamps were rinsed with acetone, dried with a nitrogen flow, and brought into contact with the IM SAMs. The μCP was performed overnight (16 hours) with 10 g weight onto the stamps with 5 and 10 μm lines and without weight with the stamps of 100 μm lines, respectively. Then, the patterned CCM substrates were rinsed with acetone and blown dry with a nitrogen flow.

Isopropanol backfilling: patterned CCM substrates were immersed in isopropanol for 1 hour and then dried with a nitrogen flow.

1-Bromo-2,2-dimethylpropane backfilling: patterned CCM substrates were immersed in a 1 mM 1-bromo-2,2-dimethylpropane solution in water for 1 hour. Then, the substrates were rinsed with MiliQ water and blown dry with a nitrogen flow.

EU SAMs: the substrates were activated in a piranha solution (H_2SO_4 and H_2O_2 3:1) for 30 minutes. Afterwards, each surface was rinsed several times with MiliQ water and dried with a

nitrogen flow. Then, the substrates were incubated in a 5 mM $EUSi(OEt)_3$ solution in dry toluene for 3.5 hours under argon. After this period of time, the substrates were dipped and rinsed with dry toluene, absolute ethanol and dichloromethane and dried with a nitrogen flow.

EUZn patterned substrates: patterned stamps were incubated by immersion in a 1 mM solution of $Zn(OAc)_2{\cdot}2H_2O$ in acetone for 1 hour. The stamps were then rinsed with acetone, dried with a nitrogen flow and brought into contact with EU SAM without weight. The printing step was performed overnight. After this time, the substrates were washed with acetone and blown dry with a nitrogen flow.

EUZnCCM patterned substrates: flat stamps were incubated in a 1 mM solution of CCM in acetone for 1 hour. The stamps were rinsed with acetone, dried with a nitrogen flow, and brought into contact with the EUZn patterned substrates without weight. The printing step was performed overnight. After this time, the substrates were rinsed with acetone and dried with a nitrogen flow.

Zn µCP: stamps were incubated in a 1 mM $Zn(OAc)_2{\cdot}2H_2O$ solution in acetone for 1 hour. Then, the stamps were brought into contact with patterned CCM substrates for 16 hours. After this time, substrates were rinsed with acetone and dried with a nitrogen flow.

Thin layer chromatography (TLC): hydrosilylation reaction was monitored by TLC, for 15 minutes, 30 minutes and 1 hour using a mixture of hexane:chloroform (8:2) and 5% of THF.

5.4. CCM-BASED SURMOFS PREPARATION

Solvothermal methodology: patterned CCM substrates with 100 µm lines and 35 µm separation pattern were placed in an upright position in a solvothermal vial. Patterned CCM substrates were previously backfilled with isopropanol. The substrates were immersed in a CCM:$Zn(OAc)_2{\cdot}2H_2O$ solution in a ratio of 1:1.78 using a solvent mixture of DEA:MeOH (1:1). The vial was closed and placed in the oven for 1 day at 85 ºC. Subsequently, the substrates were washed with MeOH by dipping or in ultrasonic bath for 3 seconds.

Drop casting: patterned CCM substrates were placed inside a vial in a flat position and 300 µL of CCM:$Zn(OAc)_2{\cdot}2H_2O$ 1:1.78 solution in DMA:MeOH 1:1 were added dropwise onto the substrate. In order to create an atmosphere of MeOH inside the vial, 300 µL of MeOH were added at the bottom of the vial. The vial was then sealed with Teflon and parafilm for 4 days at room temperature. After this time, the remaining drop on the surfaces was removed using a

pipette. The surfaces were rinsed with MeOH and dried with a nitrogen flow. The same protocol was also followed for the isopropanol or 1-bromo-2,2-dimethylpropane backfilled CCM functionalized surfaces and EU SAMs.

Layer-by-layer: patterned CCM substrates were immersed alternately in a 1 mM $Zn(OAc)_2 \cdot 2H_2O$ in DMA:MeOH (1:1) and 0.1 mM CCM in DMA:MeOH (1:1) solutions with stirring at 80 ºC for 5 minutes in each solution. Substrates were previously backfilled with isopropanol. After each cycle of immersion in the metal solution and in the CCM solution, the substrates were rinsed with MeOH and dried with a nitrogen flow. The experiments were performed up to 8 cycles of immersion in each solution.

6. SYNTHESIS

With the objective to prepare active monolayers for the preparation of curcumin-based bio-SURMOF (Figure 5c), curcumin and a derivative of the eugenol were first synthesized (Figure 5). In the case of the curcumin, the commercial curcumin available is not 100% pure and also contains desmethoxycurcumin and bisdemethoxycurcumin products, which can interfere in the crystallization of the Bio-MOF. On the other hand, a derivative of the eugenol with a reactive –$Si(OEt)_3$ group has been also prapared to funcionalize the substrates.

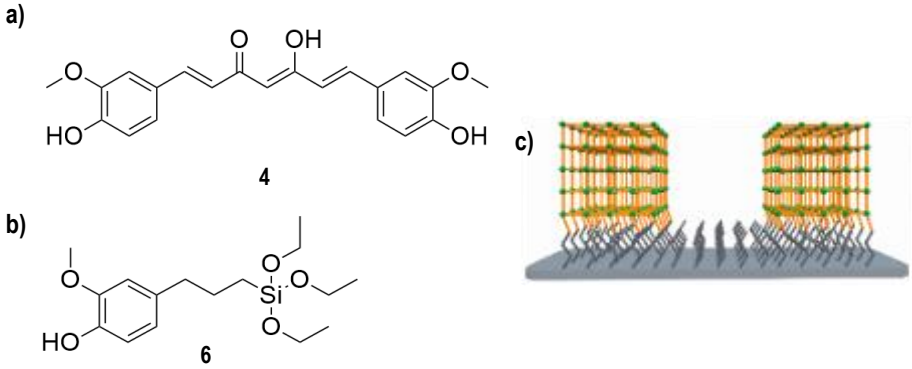

Figure 5. Structures of a) CCM (**4**), b) $EUSi(OEt)_3$ (**6**) and c) representation of the $[Zn_3(CCM)_2]$ SURMOF.

6.1. CURCUMIN SYNTHESIS (CCM)

Curcumin was synthesized following the bibliographic reported Pabon's reaction.[29] In this reaction, ethyl acetate (AcOEt) was used as a solvent, thanks to the solubility of all of the reagents in this solvent, whereas intermediates and products precipitate. Also, temperature was used to fasten the reaction, but it is not indispensable for CCM synthesis.

Initially, B_2O_3 reacts with AcAc (**1**) forming a boron complex (**2**), which is a white paste, and its formation is necessary for the subsequent aldol reaction at the methyl group of the AcAc, (Scheme 1). The formation of the boron complex is necessary to avoid the methylene deprotonation of the AcAc, and to obtain the deprotonation of the methyl groups, instead.

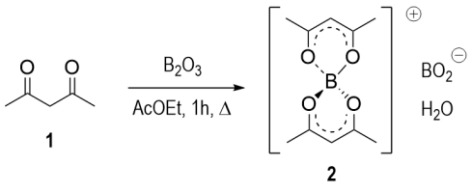

Scheme 1. Formation of the boron complex (**2**) with B_2O_3.

After the formation of the boron complex, vanillin and tributylborate were added alongside with n-butylamine. Consequently, the solution adopted a dark red colour, and the formation of the intermediate **3** is taking place (Scheme 2). Vanillin allowed the initiation of an aldol reaction, whereas tributylborate, which is a dry agent, is used to remove the water formed from the boron complex formation and from the aldol reaction. On the other hand, n-butylamine, which is a base catalyst, deprotonates the methyl group and also decreases the activation energy of the reaction. The reaction with two aldehydes did not happen at the same time. First, one vanillin equivalent reacts with a methyl group from the AcAc and the second equivalent continues the reaction with the opposite methyl group. The intermediated **3** is obtained as a dark green solid.

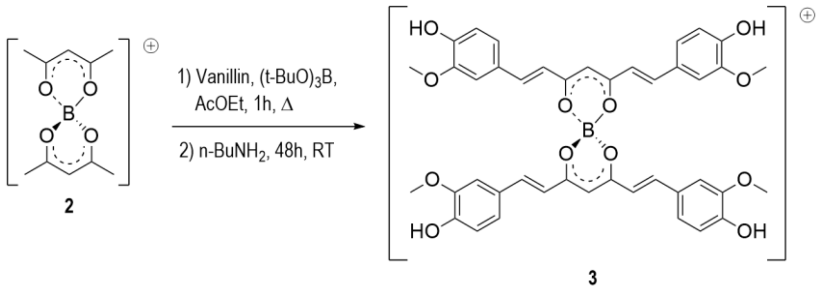

Scheme 2. Synthesis of intermediate **3**.

Finally, acid water was added to **3,** with the aim of hydrolyzing the complex and to obtain CCM (**4**,**5**) with 52 % of yield (Scheme 3) (Figure A1). Bases could also be used to decompose the complex, but CCM is unstable towards alkali media.[29].

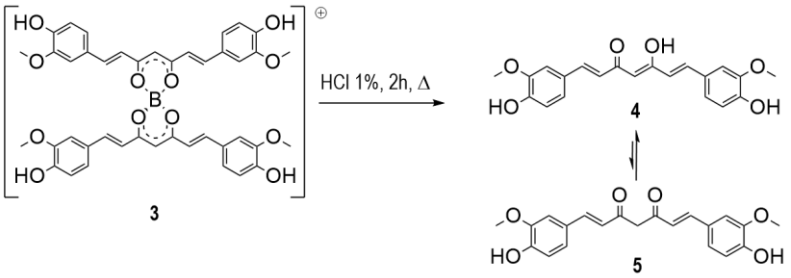

Scheme 3. Curcumin (**4**,**5**) obtention after hydrolysis with acid water.

CCM was first characterized by ^{1}H NMR. Thus, the singlets observed at 16.41 ppm and 9.67 ppm correspond to the protons of the -OH groups from the keto-enol and the aromatic groups, respectively. The singlet at 7.32 ppm corresponds to the proton in ortho position from the -OMe. Two doublets appear at 7.15 ppm and 6.82 ppm, corresponding to the protons in ortho and meta respectively from the aromatic OH, that couple between each other. The singlet at 6.05 ppm corresponds to the central proton of the CCM skeleton and the doublets at 7.55 ppm and 6.73 ppm are from the non aromatic double bonds, where the proton that shows up at higher ppm is the one next to the carbonyl group, which is electro withdrawing and reduces the shielding effect (Figure A2). In CCM structure, non aromatic double bonds have E configuration, confirmed by the coupling constants that had values of 15.6 Hz and 16.0 Hz, which are within the values of the theoretical trans coupling constant range (14-19 Hz).[31]

Secondly, the FTIR-ATR spectrum of CCM shows the different bands which can be assigned to the difrents parts of the CCM structure: at 3200-3500 cm^{-1} (O-H (ν)), 2940 cm^{-1} (C-C-H (ν)), 1632 cm^{-1} (C=C (ν)), 1594 cm^{-1} (benzene ring (ν)), 1515 cm^{-1} (C=O (ν)), 1291 cm^{-1} (aromatic C-O (ν)), 1037 cm^{-1} (C-O-C (ν)) and 959 cm^{-1} (trans C-H (δ)) (Figure A3).[32]

Finally, the optical properties of the synthesized CCM were studied by UV-Vis absorption and fluorescence emission spectroscopy. Measurements in solid and solution were performed. The solid characterization is the most remarkable because it will be used for the functionalized CCM substrates characterization.

The UV-Vis spectrum of 10^{-5} M CCM solution in CH_2Cl_2 shows two broad absorption bands. A band with the maximum at 420 nm and a second less intense absorption band with the maximum at 226 nm. On the other hand, the CCM spectrum in solid state shows a broad absorption band between 250-550 nm with its maximum absorption at 421 nm. The bands at approximately 420 nm are atributed to the to n → π* transitions from the conjugated system of the CCM skeleton, whereas the second absorption band at 226 nm corresponds to the π → π* transitions from the aromatic groups.[33]

Regarding the fluorescence spectroscopy in solid, the spectrum shows an emission peak at 573 nm (yellow region). In solution, two peaks were observed at 483 nm and 497 nm, which are the emission of the absorbance bands at 420 and 226 nm, respectively. Both emission bands lie in the blue region (Figure A4).

6.2. EUSi(OEt)$_3$ SYNTHESIS

EUSi(OEt)$_3$ (**6**) was synthesized by hydrosilylation of the allyl group of the eugenol with HSi(OEt)$_3$ (Scheme 4).[30] First of all, this reaction must be performed under argon atmosphere and protected from the light to avoid the polymeritzation of the silanes and the effectiveness of the catalyst employed, respectively. Before adding HSi(OEt)$_3$, the solution is heated up to 40 ºC in order to activate the catalyst, leading to a reaction rate raising. After HSi(OEt)$_3$ addition, the hydrosilylation took place at the β position of the allyl group, thanks to the selectivity of the Karstedt's catalyst.

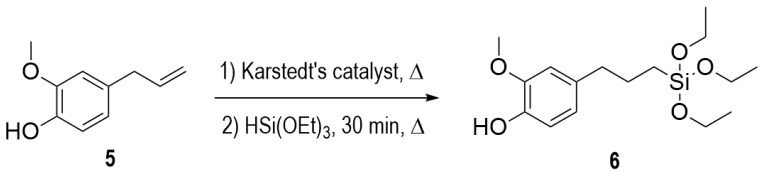

Scheme 4. EUSi(OEt)$_3$ (**6**) synthesis.

The hydrosilylation reaction was monitored by TLC, for 15 minutes, 30 minutes and 1 hour using a mixture of hexane:chloroform (8:2) and 5% of THF. The TLC showed that a huge amount of eugenol has reacted within the first 15 minutes, indicating that the reaction is really fast. After 1 hour of reaction, the final product is obtained. However, the TLC showed the presence of two singals indicating the presence of by-products, which were also confirmed by ^{1}H-NMR (Figure A5). Therefore, the reaction was finally stirred for 30 minutes, and although the

final compound obtained was still impure, the amount of the impurites was lower than for longer reaction times.

The success of the hydrosilylation reaction was also confirmed with the presence of three peaks at 0.66 (CH_2-Si), 1.71 (-CH_2) and 2.57 (Ar-CH_2) ppm, which correspond to the formation of the alkyl chain. Moreover, the peaks at 1.21 ppm and 3.80 ppm were assigned to the CH_3 and CH_2 of the –Si(OCH_2CH_3)$_3$ groups, respectively. Finally, the peaks of the impurties were assigned to the peaks at 0.07 ppm, 6.90 ppm and 1.86 pm. Although the ^{1}H-NMR spectrum showed a little amount of impurities and because they are not assigned to any silane by-product of the reaction, the EUSi(OEt)$_3$ compound was used for the preparation of the corresponding SAMs, without further purification. As for future work, the purification of EUSi(OEt)$_3$ will be performed.

On the other hand, the reaction of hydrosilylation was also monitored using FTIR-ATR, following the dissaparence of the peak at 2194 cm^{-1} corresponding to the ν_{Si-H} of the HSi(OEt)$_3$ Moreover, the FTIR-ATR spectrum of EUSi(OEt)$_3$ shows bands at 3300-3500 cm^{-1} (ν(O-H)), 2974 cm^{-1} (ν(C=C-H)), 2928 cm^{-1} (ν(C-C-H)), 1603 cm^{-1} (ν(C=C)), 1513 cm^{-1} (ν(benzene ring)) and 1071 cm^{-1} (ν(C-O-C)) (Figure A6).[34]

Finally, the UV-Vis absorption spectra of 10^{-5} M solution of EUSi(OEt)$_3$ showed a band with the maximun at 276 nm, which correspons to π → π* transitions from the aromatic group. The fluorescence spectrum showed a band with its maximum at 320 nm, which lies in the ultraviolet region (Figure A7).[35]

7. [Zn_3(CCM)$_2$] MOF IN SOLUTION

Once the CCM was synthesized, the synthesis of the [Zn_3(CCM)$_2$] MOF was performed in solution in order to reproduce the reported methodologies and to study the conditions for the further prepartion of the corresponding SURMOF. Therefore, for the obtention of [Zn_3(CCM)$_2$] MOF, solvothermal and microwave-assisted techniques were used.[36,37]

Solvothermal synthesis (ST) is a technique that takes place in a closed system and requires high temperatures close or above the boiling point of the reaction medium. This technique allows a slow crystallization in solution and has control over the size, shape and morphology of

the MOFs. Regardless, these properties are in dependance with the temperature, solvent, reaction time and ratio of the reagents, among other factors. In addition, this technique requires long reaction times and high energy consumption.[36]

Although the reported conditions for the $[Zn_3(CCM)_2]$ MOF were CCM:Zn 1:1.78 in DMA:MEOH (1:1) or DMF:EtOH (4:1)[15,20], several combinations of solvents and CCM:Zn ratios were also studied (Table 1). All the samples were incubated at 85 ºC: for 4 days.

Experiment	CCM:Zn ratio	Temperature [ºC]	Time [days]	Solvent	Volume [ml]
1	1:1.78	85	4	DMA:MeOH	2 (1:1)
2	1:1.78	85	4	DMF:MeOH	2 (1:1)
3	1:1.78	85	4	DEA:MeOH	2 (1:1)
4	1:1.78	85	4	DEA:EtOH	2 (1:1)
5	3:2	85	4	DMA:MeOH	2 (1:1)
6	1.78:1	85	4	DMA:MeOH	2 (1:1)

Table 1. Conditions for the $[Zn_3(CCM)_2]$ MOF preparation by solvothermal.

For the experiments **1** and **2**, dark red solids were obtained, which seemed to present crystals. In the case of experiments **3** and **4**, brown solids were obtained but after washing the precipiate three times with DEA:MeOH (1:1), the solid was redissolved. This can indicate that, first, the product formed could be reagents that precipitated without reacting and, second, the size of the $[Zn_3(CCM)_2]$ MOF obtained was not enough to be insoluble in the mixture of solvents, leading to its redissolution. Therefore, the results indicated that using DMA:MeOH as solvents led to the obtention of a larger amount of crystals. Consequently, this solvent mixture was fixed and the CCM:Zn ratio was modified in experiments **5** and **6**. For the synthesis of Bio-MOFs, one of the main objectives is to obtain micro or nanosized crystals for their subsequent bioapplication[15]. In the case of experiment **5,** larger crystals were obtained compared to the previous experiments, indicating that the ratio CCM:Zn was inadequate for the synthesis of $[Zn_3(CCM)_2]$ MOF. In the case of experiment **6**, a dark red solid was formed, but it did not form as many crystals as the ones obtained in experiments **1** and **2**.

The conditions used in solvothermal synthesis were employed for the $[Zn_3(CCM)_2]$ MOF synthesis in microwave-assisted (MW) technique, besides DEA:MeOH conditions. Microwave consists of an electromagnetic radiation, where the electric field is the one that transfers heat to

the sample. Microwave photons are low energy sources, meaning that they do not have enough energy to affect the structure. Microwaves couples with the molecules in solution, leading to selective heating with anything that will react with dipolar rotation or ionic conduction. For the $[Zn_3(CCM)_2]$ MOF synthesis, microwave has also been used because shorter reaction times than solvothermal methodology are necessary, less energy consumption is required and it allows to have a control over the MOF's properties such as the size, shape and morphology of the framework.[37] Four different experiments were prepared and each experiment was allowed to react at 100 ºC (Table 2).

Experiment	CCM:Zn ratio	Temperature [ºC]	Time [hours]	Solvent	Volume [ml]
7	1:1.78	100	2.5	DMA:MeOH	4 (1:1)
8	1:1.78	100	1.5	DMF:MeOH	4 (1:1)
9	1.78:1	100	3.5	DMA:MeOH	4 (1:1)
10	3:2	100	2.5	DMA:MeOH	4 (1:1)

Table 2. Conditions for the $[Zn_3(CCM)_2]$ MOF preparation by microwave-assisted approach.

For experiments **7** and **8**, red solids with certain crystallinity were obtained with 2.5 and 1.5 hours, respectively. As for expermients **9** and **10**, for both of them a dark orange solid was obtained at 3.5 and 2.5 hours, respectively.

In both experiments, using CCM:Zn 1:1.78 ratio and DMA:MeOH or DMF:MeOH as solvent mixtures led to the synthesis of some crystals, which were characterized by XRD, SEM and EDX. In addition, the EDX spectra of samples **7** and **8** demonstrated that each product formed contained Zn(II), indicating the coordination of the metal (Figure B1). Experiments with the same ratios and solvent mixtures will be compared.

All the XRD spectra of the solids obtained from the different experiments together with the theoretical one are collected in Figure 6.[15] Each experimental XRD coincide with the theoretical one, corroborating the obtention of the $[Zn_3(CCM)_2]$ MOF. The XRD spectrum of the solid of the experiment **1** (Figure 6e) shows that the solid is cristalline. However, the different intensity of the peaks can indicate a different preferencial growth of the crystal structure or the presence of a mixture of crystals. The XRD spectrum of experiment **7** (Figure 6c) shows that the solid is also crystalline with the presence of extra peaks that can indicate the presence of two different crystals. As for experiment **2** (Figure 6d), the solid obtained was the most amorphous among

the solids analysed. For the experiment **8**, high crystallinity of the solid is observed and the same preferent orientation than the other experiments (Figure 6b).

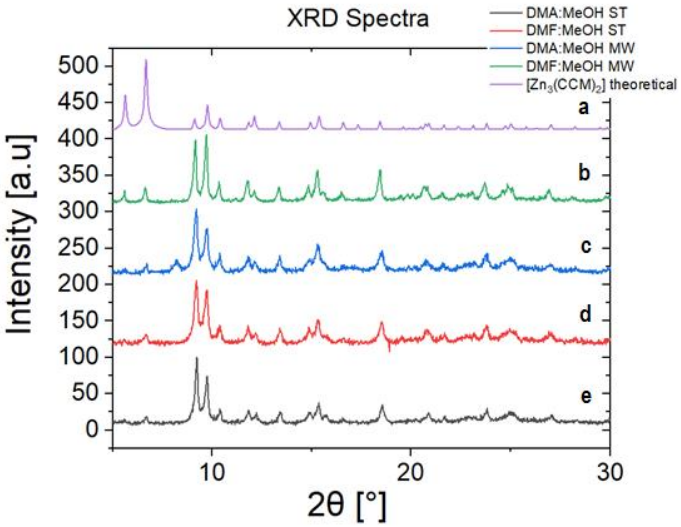

Figure 6. DRX spectra of a) theoretical $[Zn_3(CCM)_2]$ MOF[15] and of the solids obtained in the experiments b) **8**, c) **7**, d) **2** and e) **1** (ST = solvothermal, MW = microwave).

In order to confirm the morphology of the solids obtained from the different conditions, SEM characterization was carried out.

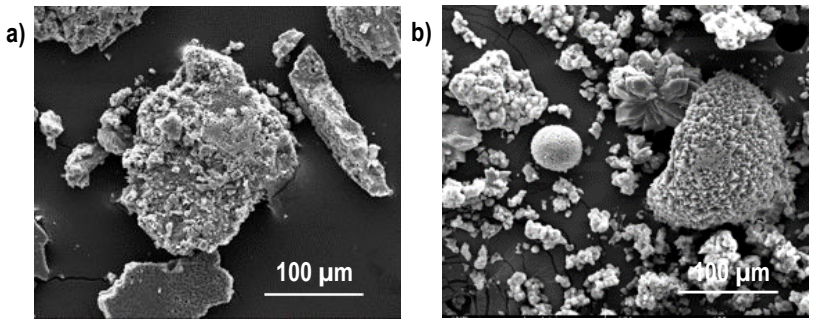

Figure 7. SEM images of experiments a) **1** and b) **7**.

By analyzing the SEM images, the solid of the experiment **1** can be microcrystalline, which explains its crystallinity, but the orientation or direction of the crystals could not be the same,

leading to the obtention of a morphology not expected for a crystalline structure (Figure 7a). On the other hand, the solid of the experiment **7** shows three different phases: crystalline flower-like shape and blocks and an amorphous solid. In addition, the flower-like crystals extend outward from the center and act as a nucleation point for the MOF growth (Figure 7b).

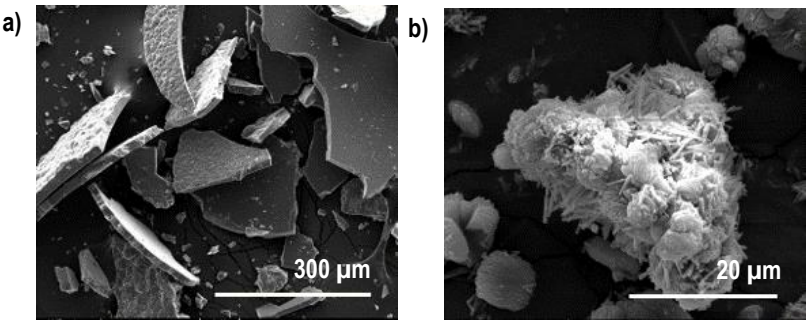

Figure 8. SEM images of experiments a) **2** and b) **8**.

The solid of the experiment **2** seems to not be as crystalline as the other samples. The SEM images shows the presence of layers of solids (Figure 8a). Finally, the image of the solid of the experiment **8** shows the formation of two phases: layered spheres and needles (Figure 8b).

8. $[Zn_3(CCM)_2]$ SURMOF

8.1. CCM-LAYER

Once the conditions of the synthesis of $[Zn_3(CCM)_2]$ MOF in solution had been stablished, the growth of the $[Zn_3(CCM)_2]$ SURMOF will be attempted under the same conditions. For the growth of a SURMOF, one strategy is to use a functionalization surface, in this work, a functionalized glass substrate in order to characterize it via fluorescence. The growth of the $[Zn_3(CCM)_2]$ SURMOF starts with the preparation of patterned CCM substrates in specific locations. For this purpose, micro-contact printing (µCP) was used. This technique consists in the preparation of PDMS stamps, which present a line pattern, and the further incubation with

the molecule that is going to be immobilized. For the preparation of the patterned CCM substrates, the strategy is summarized in Figure 9.

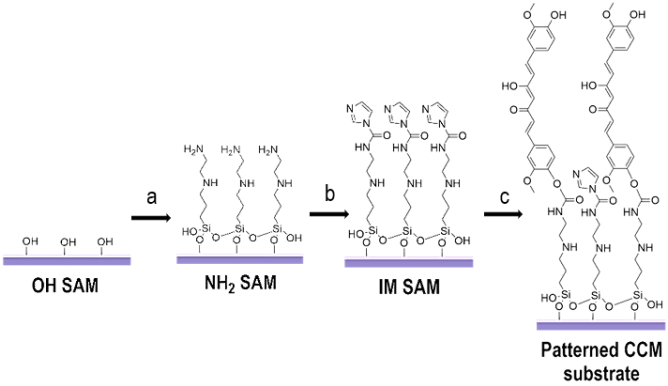

Figure 9. Scheme of the different steps to obtain a patterned CCM substrate: a) vapour deposition of TPEDA, b) immersion in CDI solution and c) μCP of CCM.

First, the glass surface was activated by immersion in an acid piranha solution with the aim of cleaning organic residues off the surface and create OH terminal groups. Once the OH SAM was accomplished, NH_2 SAM was prepared by vapour deposition of TPEDA. NH_2 SAM must be washed with absolute ethanol and dichlorometane in order to remove physisorbed silanes and water residues from the surface, respectively (Figure 9a). Then, the IM SAM was obtained by immersion in a saturated CDI solution, subsequently washed with dry THF to remove any CDI residue (Figure 9b).[38] Afterwards, μCP of CCM was performed on the IM SAM (Figure 9c), reacting through the OH groups of the CCM forming an amide covalent bond. It is expected that the phenol groups will mainly react with the IM SAM rather than the enol group because they are more nucleophilic.

The different SAMs were characterized by contact angle measurements, fluorescence microscopy and XPS. The contact angle measurements of all the SAMs are presented in Table 3. When the OH SAM was functionalized with TPEDA, the surface became hydrophobic due to the increase in number of carbon atoms of the chain from the NH_2 SAM. Once the IM SAM was obtained, the contact angle decreased due to the presence of polar atoms in the terminal imidazole chain. Finally, for the patterned CCM substrate, the contact angle increased due to the low polarity that CCM presents (Table 3) (Table B1, theoretical contact angles).

Substrate (Glass)	Θ_S (°)	Θ_A (°)	Θ_R (°)
OH SAM	8 ± 1	13 ± 3	8 ± 8
NH_2 SAM	73 ± 1	71 ± 5	62 ± 7
IM SAM	68 ± 1	64 ± 3	51 ± 7
CCM substrate	76 ± 1	74 ± 4	61 ± 10

Table 3. Contact angle measurements of functionalized glass surfaces via static (Θ_S), advancing (Θ_A) and receding (Θ_R) contact angles.

Fluorescence controls were performed on NH_2 SAM and IM SAM by µCP, using 5 µm lines with 10 µm separation patterned stamps (5 x 10 µm), and employing different inking solutions: 1 mM solution of Rhodamine B isothiocyanate (RITC) for the NH_2 SAM and 1 mM solution of 6-aminofluorescein (6-AF) for the IM SAM, using MeOH as a solvent in both solutions. RITC and 6-AF are well known dyes with a high quantum yield. In the case of the NH_2 SAM the isothiocyanate group of RITC molecule reacted with the terminal amine group, obtaining red patterns upon the printing (Figure 10a). For the IM SAM, the amine group of 6-AF reacted with the terminal imidazole group of the IM SAM (Figure 10b).

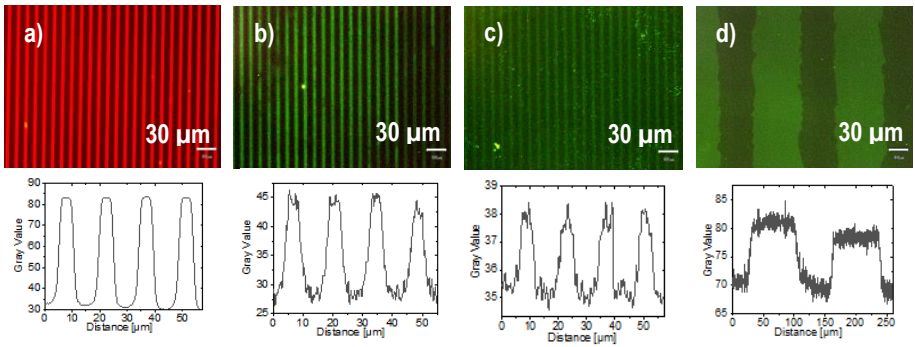

Figure 10. Fluorescence microscopy images of a) RITC µCP on NH_2 SAM with not oxidized patterned stamp of 5 x 10 µm, b) 6-AF µCP on IM SAM with 5 minute oxidized patterned stamp of 5 x 10 µm, CCM substrates with c) 5 x 10 µm pattern using 5 minute oxidized stamp and d) 100 x 35 µm pattern using 10 minute oxidized stamp. (Scale bar 30 µm, aperture 8, ImageJ software, excitation filter: 450 nm ≤ λ_{ex} ≤ 480 nm; Emission filter: λ_{em} ≥ 515 nm).

To confirm the formation of each SAM, XPS was used with functionalized Si-wafers. C1s region of NH_2 SAM shows peaks at 285.43, 287.27, 290.08 and 293.07 eV corresponding to C-C/C-H/C-Si, C-N/C-O, C=O and π-π* satellite, corroborating the formation of the NH_2 SAM. As for the IM SAM, measurement in C1s region shows peaks at 287.97 and 288.9 eV, which corresponded to N-C(O)-N and N-C-N peaks, confirming the formation of the imidazole monolayer.[38] In addition, the N1s spectrum shows peaks at 400.86 and 401.93 eV denoting N-H/N=C and N-C bonds. Regarding the CCM SAM, the abundance of nitrogen has been lowered comparing to the IM SAM. This is explained by the fact that the N=C bond from the imidazole is not present anymore, leading to a reduction of the amount of nitrogen in the sample (Figure B2).[39-41]

Although it has been demonstrated that the CDI molecule reacts with the amine terminated monolayer forming the IM SAM, some precautions are important to take into consideration. Since CDI decomposes immediately in contact with water, forming CO_2 and two imidazole groups[42], argon atmosphere is required for this reaction. Therefore, the immersion time of the NH_2 SAM in the saturated CDI solution is crucial. Different fluorescence tests were carried out by immersing the NH_2 SAM for 4 and 24 hours in order to optimize the subsequent CCM μCP.

After the CCM μCP, fluorescence patterns were obtained for both IM SAMs. However, for the 24 hour incubation time, the pattern presented lower fluorescence, indicating a possible decomposition of the IM SAM. As a conclusion, immersing the NH_2 SAM in the CDI solution for 4 hours is enough time to have an important number of imidazole groups and react with the CCM (Figure B3).

Once the NH_2 SAM immersion time was optimized, the conditions for the printing of CCM were also optimized. The μCP method is influenced by several factors, including stamp oxidation, the stamp inking and μCP times and the weight applied onto the stamp when performing the μCP. Therefore, different parameters were studied and the fluorescence of CCM patterns was checked.

The first test consisted in oxidizing 5 x 10 μm and 100 μm lines with 35 μm separation (100 x 35 μm) patterned stamps for 5 and 10 minutes. When the PDMS stamp is oxidized, the terminal methyl groups are replaced with hydroxyl groups, increasing the polarity and the energy surface, therefore a better attachment of the molecule. This is the case of 10 minutes oxidized 100 x 35 μm stamps (Figure 10d). By oxidizing for 5 minutes, the pattern is barely

visible because the oxidation is not enough for the CCM to attach. Regardless, if the oxidation is too aggressive, the destruction of the patten takes place, which is the case of 10 minute oxidized 5 x 10 µm stamps (Figure B3). Only a small CCM patten spot is seen all over the substrate, whereas 5 minute oxidized 5 x 10 µm stamp leads to the formation of all the pattern (Figure 10c). Stamps with 10 µm lines with 20 µm separation (10 x 20 µm) pattern show great results by oxidating them for 5 minutes, therefore no modifications were done (Figure B3).

Regarding the inking process of the stamps in CCM and the µCP times, they were performed for 1 hour and 16 hours, respectively. These times allowed the observation of good patterns with good signal:noise ratio with high reproducibility of the patterns. These long times used indicated that the interaction between the CCM and the stamp is not strong and that its reaction with the IM SAM is slow.

In order to check if Zn(II) coordinates with CCM, XPS technique was performed on a CCM functionalized Si-wafer. After the coordination of Zn(II) to CCM SAM, the XPS spectra shows a Zn2p region with peaks at 1045.99 and 1023.11 eV, which corresponded to Zn2p1/2 and Zn2p3/2, respectively (Figure B4).[43]

Once the patterned CCM substrate was prepared, the selectivity of the patterns towards the growth of the SURMOFs was tested by immersion of the surface in a 1 mM solution of CCM and $Zn(OAc)_2 \cdot 2H_2O$ in acetone overnight (Figure 11a). The optical microscope image showed that the crystals did not grow following the pattern, therefore the procedure must be optimized. The reason why crystals grew without following any order is because the not patterned area has terminal imidazole groups that did not react. These groups contain nitrogen atoms where the Zn can coordinate to, therefore not only the SURMOF can grow from the CCM pattern but also from the not patterned area.

To prevent the SURMOF growth out of the pattern, a backfilling step was performed. Backfilling is the passivation process of the areas where the CCM was not stamped. Isopropanol was first employed to perform the backfilling. The terminal imidazole groups, which are good leaving groups, can be replaced with isopropanol forming a terminal ester. The 10 x 20 µm patterned CCM substrates were immersed in isopropanol for 1 hour and a fluorescence control was performed (Figure 11b). After executing the backfilling for 60 minutes, the fluorescence decreased (Figure 11c). There are several reasons that could have produced the fluorescence decrease.

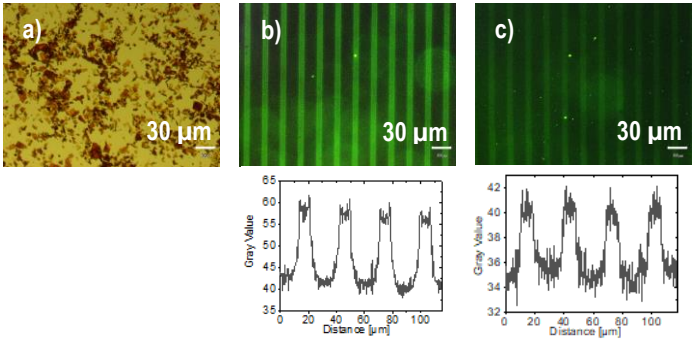

Figure 11. a) Crystal formation onto CCM substrate after the immersion in 1 mM solution of CCM and $Zn(OAc)_2 \cdot 2H_2O$ and 10 x 20 µm patterned CCM substrates (aperture 1/2.5) b) before and c) after isopropanol backfilling (Scale bar 30 µm, aperture 8, ImageJ software).

One reason would be that there are some CCM molecules that are not fully anchored onto the surface, hence the isopropanol solution can remove them, resulting in a florescence loss. In addition, some imidazole groups could have not reacted in the area where the CCM was stamped because of the hinderance that CCM produces, thus the fluorescence will also decrease in the printed areas after the backfilling. Moreover, the static contact angle (Θ_S) of the IM SAM was performed before and after backfilling. The angle increased from 68 ° ± 1 to 82 ° ± 1, leading to a more hydrophobic surface due to the terminal ester and resulting in a successful backfilling.

Once the backfilling was achieved, three different techniques were developed with the aim of growing the $[Zn_3(CCM)_2]$ SURMOF onto the surface: layer-by-layer, drop casting and solvothermal. The optimized conditions for the preparation of the MOFs in solution were then used to prepare the $[Zn_3(CCM)_2]$ SURMOF, with that handicap that some of the conditions that work for MOFs in solution could not work for their growth onto a surface because some factors are different, as the interaction of the surface with the environment.

The layer-by-layer strategy (LBL) allows the growth of SURMOFs by allowing the substrate to undergo several cycles of immersion in the metal ion solution followed by the immersion in the organic ligand solution, or vice versa, and rinsing the surfaces after each immersion. Theoretically, a monolayer is formed after each cycle, therefore the SURMOF is grown onto the substrate under control. In addition, there are several factors such as temperature, time and solvent that need to be considered beforehand when performing layer-by-layer technique.[44]

Therefore, a CCM substrate with 5 x 10 µm pattern was immersed in isopropanol for 1 hour and was used to perform the layer-by-layer strategy. Eight cycles of ten minutes were performed (5 minutes in 1 mM $Zn(OAc)_2 \cdot 2H_2O$ solution and 5 minutes in 0.1 mM CCM solution) and temperature (80 ºC) was applied because it is reported that the $[Zn_3(CCM)_2]$ MOF forms at 80 ºC.[20] After performing 3 cycles, the surface shows a subtle pattern and the lines become more pronounced after each cycle is performed (Figure 12a). It seems that the nucleation process is taking place and, in order to form crystals onto the pattern, more cycles could be performed, or the immersion time could be increased.

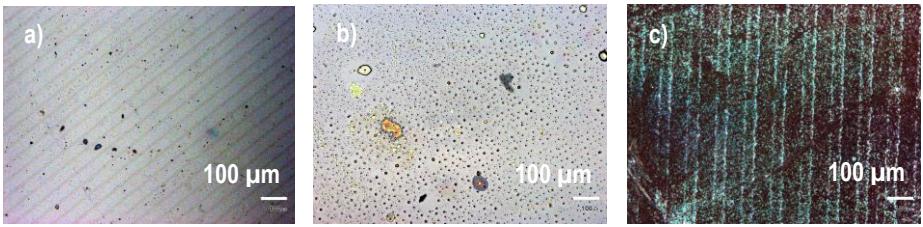

Figure 12. Microscope images of CCM substrates with a) 5 x 10 µm pattern from LBL, b) 10 x 20 µm from DC and c) 100 x 35 µm from ST (Scale bar 100 µm, aperture 1/60).

The simplest method for the deposition of a MOF on a patterned surface is by drop casting (DC). This method is employed to crystallize the SURMOF, where a solution containing the reagents is added dropwise onto the micropatterned surface and the solvent is added dropwise at the bottom of the vial. Consequently, the equilibrium liquid-gas takes place, forcing the crystal formation by solvent evaporation.[45]

As for this strategy, a CCM substrate with 10 x 20 µm pattern was used and immersed in isopropanol for 1 hour. 300 µL of CCM:$Zn(OAc)_2 \cdot 2H_2O$ 1:1.78 solution in DMA:MeOH 1:1 were added dropwise onto the substrate, meanwhile 300 µL of MeOH were added at the bottom of the vial. After 4 days of reaction, the surface formed small crystals following a pattern, meaning that the passivation was successful and confirming the selective growth of the $[Zn_3(CCM)_2]$ SURMOF. (Figure 12b).

For the solvothermal technique (ST), a CCM substrate with 100 x 35 µm pattern was used and immersed in isopropanol for 1 hour. The substrate was then put in a vial, using DEA:MeOH (1:1) as solvents and a ratio of 1:1.78 CCM:Zn, and left reacting for 1 day. After this time, the optical microscope image showed that some crystals grew out of the CCM lines (Figure 12c),

leading to the conclusion that there could be another terminal group that did not react and was not taken into consideration.

Terminal amine groups from the NH_2 SAM might not have reacted with the CDI afterwards because of the hinderance, meaning that the Zn(II) could have coordinated and, therefore, the SURMOF could have grown. In order to prevent this, the amine groups were alkylated with a compound with hinderance, hence avoiding polyalkylation. The compound used was 1-bromo-2,2-dimethylpropane, dissolved in water (1 mM solution).

Three different NH_2 SAMs were immersed in water (Figure 13b) and in 1-bromo-2,2-dimethylpropane (Figure 13c) for 1 hour and not immersed (Figure 13a), respectively, with the aim of checking if the bromo compound alkylates the amine groups as expected or if water can affect the substrate. The substrates were characterized via fluorescence microscopy and contact angle measurements.

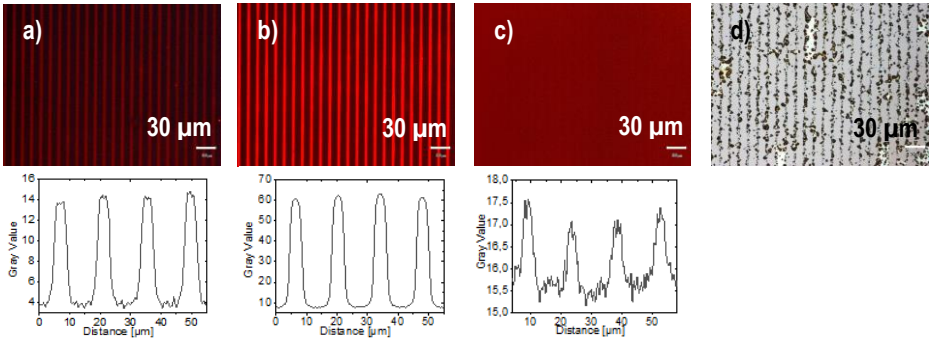

Figure 13. Fluorescence images of NH_2 SAMs patterned with RITC after a) no backfilling, b) immersing in water and c) immersing in 1-bromo-2,2-dimethylpropane (Aperture 8, ImageJ software). Microscope image of d) $[Zn_3(CCM)_2]$ SURMOF substrate from DC (Aperture 1/60, scale bar 30 µm).

NH_2 SAMs were immersed for 1 hour in their respective solutions. Then, a µCP with RITC was performed. After immersing the NH_2 SAM in water, the RITC perfectly reacts with amine groups, meaning that water does not affect these groups. Also, the stripes experience an increase of the fluorescence. Removing water completely is difficult, so if the substrate is not fully dried, water can retain more RITC molecules resulting in more fluorescence intensity (Figure 13b). As for the NH_2 SAM immersed in 1-bromo-2,2-dimethylpropane, the alkylation of the amines is successful because, if amines are alkylated, RITC molecules cannot react, leading to no pattern formation (Figure 13c). The amine groups were being alkylated, therefore

fluorescent patterns were not observed, indicating the successful blocking of the NH_2 SAM. Contact angle measurements were also performed to verify if amine groups had been alkylated (Table 4).

Surface (Glass)	Θ_S (°)
NH_2 SAM	70 ± 1
NH_2 SAM + H_2O	72 ± 1
NH_2 SAM + Br	76 ± 1

Table 4. Static contact angles of different NH_2 SAMs.

After immersing the NH_2 SAM in water, the contact angle was slightly higher, but the difference is within the error range. In comparison, the substrate immersed in 1 mM solution of 1-bromo-2,2-dimethylpropane increased the contact angle. The amine groups are being alkylated, leading to a more hydrophobic surface and a higher contact angle value.

After achieving the alkylation of the amines, drop casting methodology was performed to check if the SURMOF can grow selectively. The substrate was immersed in isopropanol and in 1 mM 1-bromo-2,2-dimethylpropane solution for 1 hour each and the same drop casting procedure was performed. After reacting for 4 days, crystals were formed following the pattern perfectly, meaning that a combination of both passivation procedures and that the crystals grew onto the CCM patterns, which act as nucleation points (Figure 13d). Knowing that the crystals grew following the pattern, solvothermal and layer-by-layer techniques will be performed as for future work. The obtained patterned substrates were analysed via SEM in order to check the morphology of the solid growth on the patterns (Figure 14).

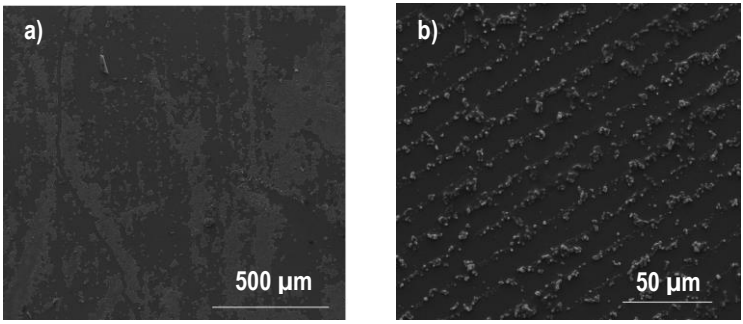

Figure 14. SEM images of a) isopropanol backfilled substrate obtained via solvothermal and b) isopropanol and 1-bromo-2,2-dimethylpropane backfilled substrate obtained via drop casting.

The surface obtained from the layer-by-layer technique was not analysed by SEM because the pattern could not be seen with the optical microscope. For the solvothermal methodology, the SEM image presents the formation of solid, with amorphous appearance, following a pattern in some areas of the substrate (Figure 14a). On the other hand, the surface used for the drop casting methodology shows crystals specifically located on the CCM patterns, which could be crystals of $[Zn_3(CCM)_2]$ (Figure 14b). The EDX spectrum corroborated the presence of Zn(II) in the crystals but with low intensity due to their small size (Figure B5). In order to confirm if the $[Zn_3(CCM)_2]$ SURMOF has been formed, XRD analysis could be performed on the surfaces.

8.2. EU-LAYER

When synthesizing Bio-MOFs, the biocompatibility and the interaction between the Bio-MOF and the living organism need to be considered.[4] One of the factors that influences the biocompatibility of a Bio-MOF is the crystal size: larger crystals can lead to serious toxicity issues, therefore the crystal size must be reduced. The use of capping ligands has been a strategy described in literature to reduce the size of the CCM Bio-MOF.[15]

Therefore, the preparation of eugenol-based monolayers (EU-layer) has been explored as alternative monolayer to grow the SURMOF and also reduce its size. This strategy consists in the covalent attachment of $EUSi(OEt)_3$ molecules onto a terminal hydroxyl monolayer followed by the μCP of Zn(II) (Figure 15), where CCM coordinates to, leading to the growth of the $[Zn_3(CCM)_2]$ SURMOF.

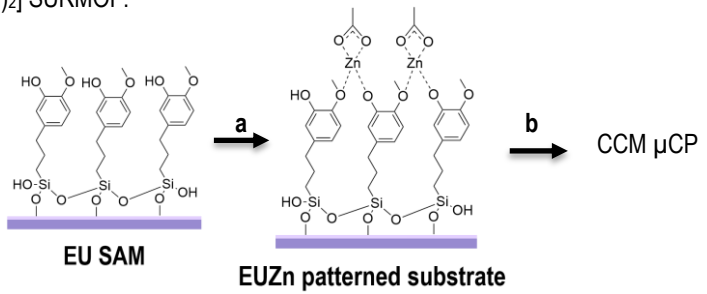

Figure 15. Functionalization process of a) EU SAM via μCP of Zn(II) forming EUZn patterned substrate and b) CCM μCP onto EUZn patterned substrate.

The formation of the EU SAM was indirectly confirmed using fluorescence microscope. For this, first Zn(II) ions were patterned on the EU SAM, and the EUZn patterned substrate was then

printed with CCM. The μCP of Zn(II) was performed onto the activated $EUSi(OEt)_3$ monolayer (EU SAM) overnight using a 10 x 20 μm patterned stamp (Figure 15a). Then, a flat stamp inked with CCM was brought into contact with the EUZn patterned SAM overnight (Figure 15b). Consequently, when the substrate was analysed by fluorescence microscopy, fluorescence patterns were obtained due to the coordination of the CCM with the Zn(II), hence confirming the EU SAM formation and the coordination of Zn(II) (EUZn patterned substrate) and CCM (EUZnCCM patterned substrate) (Figure 16a).

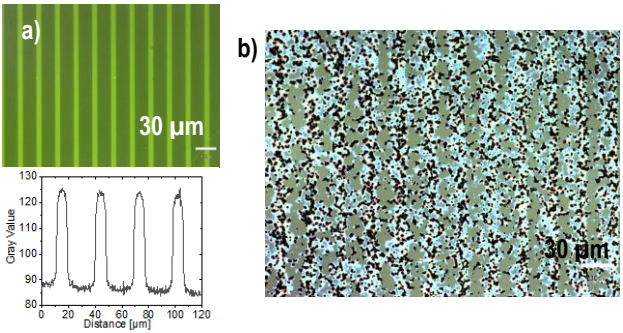

Figure 16. Fluorescence image of a) EUZnCCM 10 x 20 μm patterned substrate (aperture 8, ImageJ software) and optical microscope image of b) crystals of $[Zn_3(CCM)_2]$ formed by drop casting on 10 x 20 μm patterns of EUZnCCM (aperture 1/60, scale 30 μm).

Contact angle measurements on Si wafers were performed to confirm the formation of the monolayers. EU SAM presents a static angle of 46 º and, after the coordination Zn(II), the contact angle increases. The substrate becomes more hydrophobic due to the acetate group of $Zn(OAc)_2{\cdot}2H_2O$. After the coordination of the CCM onto the EUZn patterned substrate, the static contact angle is similar. However, the corresponding advancing and receding contact angles increased due to the low polarity that CCM structure presents (Table 5). Therefore, the functionalization of the substrates has been accomplished.

Surface (Si wafer)	Θ_S (º)	Θ_A (º)	Θ_R (º)
EU SAM	46 ± 1	49 ± 4	47 ± 7
EUZn substrate	73 ± 1	70 ± 5	53 ± 12
EUZnCCM substrate	71 ± 1	89 ± 3	67 ± 5

Table 5. Contact angle measurements of functionalized Si wafers via static (Θ_S), advancing (Θ_A) and receding (Θ_R) contact angles.

XPS spectra were performed using functionalized silicon oxide substrates to confirm the success of every functionalized surface. Regarding the EU SAM, measurements in the C1s region showed bands at 285.46, 287.20 and 289.45 eV, which corresponded to C-H/C-Si/C-C/C=C, C-O and C=O. Once the EU SAM was printed with Zn(II) (EUZn SAM), the XPS spectrum showed a Zn2p region with peaks at 1047.06 and 1023.72 eV, which corresponded to Zn2p1/2 and Zn2p3/2, respectively. After measuring the EUZnCCM SAM no new bands were formed but the spectrum shows an increment in intensity of carbons, which can be attributed to the presence of the curcumin. (Figure B5).[39-41,43]

Finally, the growth of the [$Zn_3(CCM)_2$] SURMOF on the EUZn monolayer by drop casting was studied. However, because the EU SAM was micropatterned with Zn(II), terminal OH and OCH_3 groups from the EU SAM are still present and they can influence the selectivity of the EUZn patterns towards the SURMOF. To avoid this, a backfilling step with 1-bromo-2,2-dimethylpropane was performed. Since this process is an alkylation of the OH groups, no pattern was seen by fluorescence microscopy.

EUZn patterned substrate was backfilled for an hour in a 1 mM solution of 1-bromo-2,2-dimethylpropane. Once the backfilling was finished, the substrate was incubated by drop casting methodology for 4 days and crystals on the pattern were selectively grown, corroborating that the OH groups had been alkylated (Figure 16b).

Knowing that the crystals grew following the pattern, solvothermal and layer-by-layer methodologies will be performed as for future work.

9. CONCLUSIONS

Regarding the $[Zn_3(CCM)_2]$ MOF synthesis in solution, starting from the same reagents does not lead to the same final product in terms of morphology. Even though the same CCM:Zn ratio or mix of solvents are used in solvothermal and microwave-assisted methodologies, products differ from morphology between each other due to the conditions of each technique. Regardless, the crystal structure of the solids obtained is the same, which was confirmed via XRD. In addition, the results from the different experiments, which present different phases of crystals, indicate that the procedures need to be optimized.

Immersing the IM SAM for longer periods of time leads to the decomposition of more terminal imidazole groups, leading to a worse attachment of CCM onto the IM SAM, and therefore lower quality CCM monolayers. Also, the oxidation time of the stamp interferes in the μCP process, resulting in a better attachment of CCM or the destruction of the pattern depending on the patterned stamp used and the oxidation time. In the case of the EU SAM, its formation and reactivity with Zn(II) has been proved by the appearance of fluorescent patterns when CCM was printed onto the metal functionalized surfaces.

For the selective SURMOF growth on the CCM monolayers and EU SAMs, a backfilling step of the non-patterned areas is necessary. From the two different backfilling agents used better results have been obtained with the 1-bromo-2,2-dimethylpropane and crystals were observed only on the corresponding CCM and EUZn patterns, respectively.

Three different methodologies for the $[Zn_3(CCM)_2]$ SURMOF growth have been developed. For both reactive monolayers, the drop-casting approach has allowed the visualization of selectively crystals growth. However, it is still necessary further characterization to determine their composition.

10. REFERENCES AND NOTES

1. Xuechao, C.; Zhongxi, X.; Dandan, L. Nano-sized metal-organic frameworks: Synthesis and applications. *Coord. Chem. Rev.* **2020**, *417,* 1-21.
2. Yuan, Z.; Zhang, L.; Shaozhou, L. Paving Metal-Organic Frameworks with Upconversion Nanoparticles via Self-Assembly. *J. Am. Chem. Soc.* **2018**, *140*, 15507-15515.
3. Morozova, S. M.; Sharsheeva, A.; Morozov, M. I. Bioresponsive metal-organic frameworks: Rational design and functions. *Coord. Chem. Rev.* **2021**, *431*, 1-28.
4. Rojas, S.; Devic, T.; Horcajada, P. Metal organic frameworks based on bioactive components. *J. Mater. Chem. B.* **2017**, *5*, 2560-2573.
5. Redfern, L. R.; Farha, O. K. Mechanical properties of metal-organic frameworks. *Chem. Sci.* **2019**, *10*, 10666-10679.
6. Tibbetts, I.; Kostakis, G. E. Recent Bio-Advances in Metal-Organic Frameworks. *Molecules*. **2021**, *25, 1-32.*
7. Lihiu, W.; Sumin, G.; Jing, B. Enzyme immobilized in BioMOFs: Facile synthesis and improved catalytic performance. *Int. J. Biol. Macromol.* **2020**, *144*, 19-28.
8. Butova, V. V.; Soldatov, M. A.; Guda, A. A. Metal-organic frameworks: structure, properties, methods of synthesis and characterization. *Russ. Chem. Rev.* **2016**, *85*, 280.
9. Hong, C.; Yong-Liang, H.; Dan, L. Biological metal-organic frameworks: Structures, host-guest chemistry and bio-applications. *Coord. Chem. Rev.* **2019**, *378*, 207-221.
10. Giles-Mazón, E. A.; Germán-Ramos, I. Synthesis and characterization of a Bio-MOF based on mixed adeninate/tricarboxylate ligand and zinc ions. *Inorganica Chim. Acta.* **2018**, *469*, 306-311.
11. Portolés-Gil, N.; Lanza, A.; Aliaga-Alcalde, N. Crystalline Curcumin bioMOF Obtained by Precipitation in Supercritical CO_2 and Structural Determination by Electron Diffraction Tomography. **2018**, *6*, 12309-12319.
12. Stock, N.; Biswas, S. Synthesis of Metal-Organic Frameworks (MOFs): Routes to Various MOF Topologies, Morphologies, and Composites. *Chem. Rev.* **2012,** *112*, 933-969.
13. Rojas, S.; Arenas-Vivo, A.; Horcajada, P. Metal-organic frameworks: A novel platform for combined advanced therapies. *Coord. Chem. Rev.* **2019,** *388*, 202-206.
14. Ma, P.; Jinglin, Z.; Ping, L. Computer-assisted design for stable and porous metal-organic framework (MOF) as a carrier for curcumin delivery. *LWT – Food Science and Technology.* **2020**, *120* 1-7.
15. Xiaodong, F., Yufei, W.; Faheem, M. Size, Shape, and Porosity Control of Medi-MOF-1 via Growth Modulation under Microwave Heating. *Cryst. Growth Des.* ***2019****, 19,* 889–895.
16. Guohuan, H.; Yuping, Y. Curcumin-loaded nanoMOFS@CMFP: A biological preserving paste with antibacterial properties and long-acting, controllable release. *Food Chem.* **2021,** *337*, 1-9.
17. Moussa, Z.; Hmadeh, M. Encapsulation of curcumin in cyclodextrin-metal organic frameworks: Dissociation of loaded CD-MOFs enhances stability of curcumin. *Food. Chem.* **2016,** *212,* 485-494.
18. González-Albadalejo, J.; Sanz, D. Curcumin and curcuminoids: Chemistry, structural studies and biological properties. *An. Real. Acad. Nal*. Farm. **2015,** *81*, *278-310.*
19. Pedersen, U.; Rasmussen, P.B. Synthesis of Naturally Occurring Curcuminoids and Related Compounds. *Liebigs Ann. Chem.* **1985,** *1557-1569.*
20. Hongmin, S.; Fuxing, S. A highly porous medical metal-organic framework constructed from bioactive curcumin. *Chem. Commun.* ***2015,*** *51,* 5774-5777.

21. Bétard, A; Fischer, R. A. Metal-Organic Framework Thin Films: From Fundamental to Applications. *Chem. Rev.* **2012**, *112,* 1055-1083.
22. Liu, J. et al. Surface-supported metal-organic framework thin films: fabrication methods, applications and challenged. *Chem. Soc. Rev.* **2017**, *46,* 5730.
23. Singh, M.; Kaur, N. The role of self-assembled monolayers in electronic devices. *J. Master. Chem. C.* **2020,** *8,* 2938-3955.
24. Hasan, A; Pandey, L. M. Self-assembled monolayers in biomaterials. *Nanobiomaterials.* **2018,** 138-178.
25. Käfer, D.; Witte, G. A Comprehensive Study of Self-Assembled Monolayers of Anthracenethiol on Gold: Solvent Effects, Structure, and Stability. *J. Am. Chem. Soc.* **2006,** *128,* 1723-1732.
26. Parra Vello, T; Strauss, M. Deterministic control of surface mounted metal-organic framework growth orientation on metallic and insulating surfaces. *Phys. Chem. Chem. Phys.* **2020***, 22*, 5839-5846.
27. Perl, A.; Reinhoudt, D. N. Microcontact Printing: Limitations and Achievements. *Adv. Mater*. **2009**, *21*, 2257-2268.
28. Lamping, S.; Buten, C. Functionalization and Patterning of Self-Assembled Monolayers and Polymer Brushes Using Microcontact Chemistry. *Acc. Chem. Res.* **2019**, *52*, 1336-1346.
29. Pabon, H. J. J. A synthesis of curcumin and related compounds. *Recl. Trav. Chim*. Pays-Bas. **1964**, *83*, 379-386.
30. Pillot, J-P; Birot, M. The use or naturally-occurring phenols in the synthesis of novel functional polysiloxanes. *Surf. Coating Int. B Coating Trans.* **2001**, *84*, 169-242.
31. Pretsch, E; Bühlmann, P. *Structure Determination of Organic Compounds*, 4th ed.; Springer, 2009.
32. Dang, Y. T. et al. Room temperature synthesis of biocompatible nano Zn-MOF for the rapid and selective adsorption of curcumin. *J. Sci. Adv. Mater. Devices*. **2020**, *5*, 560-565.
33. Aliaga-Alcalde, N. et al. Copper curcuminoids containing anthracene groups: fluorescent molecules with cytotoxic activity. *Inorg. Chem*. **2010**, *49*, 9655–9663.
34. Makuch, E.; Nowak, A. Enhancement of the antioxidant and skin permeation properties of eugenol by the esterification of eugenol to new derivatives. *AMB Expr.* **2020**, *10*, 1-15.
35. Vespe, V. C.; Boltz, D. F. Ultraviolet Spectrophotometric Study of Eugenol-Isoeugenol System. *Anal. Chem.* **1952**, *24*, 664-666.
36. Walton, R. I. Subcritical solvothermal synthesis of condensed inorganic materials. *Chem. Soc. Rev.* **2002**, *31*, 230-238.
37. Sun, Y.; Zhou, H-C. Recent progress in the synthesis of metal-organic frameworks. *Sci. Technol. Adv. Mater.* **2015**, *16,* 1-11.
38. Hsu, SH; Reinhoudt, D. N. Imidazole monolayers for reactive microcontact printing. *J. Mater. Chem.* **2008**, *18*, 4959-4963.
39. Bou, M. et al. Chemistry of the interface between aluminium and polyethyleneterephthalate by XPS. *Appl. Surf. Sci.* **1991***, 47,* 149-161.
40. Yan, X. et al. Prparation and characterization of electrochemically deposited carbon nitride films on silicon substrate. *J. Phys. D: Appl. Phys.* **2004***, 37,* 907-913.
41. M. Y. Bashouti. et al. Silicon nanowires terminated with methyl functionalities exhibit stronger Si-C bonds equivalent 2D surfaces. *Phys. Chem. Chem. Phys.* **2009***, 11,* 3845-3848.
42. Engstrom, K. M. The Stability of N,N-Carbonyldiimidazole Toward Atmospheric Moisture. *Org. Process Res. Dev.* **2014***, 18*, 488-494.
43. Xu, D. et. al. Catalyst-free direct vapour-phase growth of $Zn_{1-x}C_xO$ micro-cross structures and their optical properties. *Nanoscale Res. Lett*. **2013**, *8*, 1-9.
44. Summerfield, A; Cebula, M. Nucleation and early stages of layer-by-layer growth of MOFs on surfaces. *J. Phys. Chem.* **2015**, *119*, 23544−23551.
45. Ameloot, R.; Gobechiya, E. Direct Patterning of Oriented Metal–Organic Framework Crystals via Control over Crystallization Kinetics in Clear Precursor Solutions. *Adv. Mater.* **2010**, *22*, 2685-2688.

11. ACRONYMS

^{1}H NMR: Proton nuclear magnetic resonance.

6-AF: 6-aminofluorescein.

AcAc: Acetylacetonate.

AcOEt: Ethyl acetate.

Bio-MOF: Biological Metal-Organic Framework.

CCM: Curcumin.

$CDCl_3$: Deuterated chloroform.

CDI: N,N-carbonyldiimidazole.

CH_2Cl_2: Dichloromethane.

DC: Drop casting.

DEA: N,N-Diethylacetamide.

DMA: N,N-Dimethylacetamide.

DMF: Dimethylformamide.

DMSO-d_6: Deuterated dimethyl sulfoxide.

EDX: Energy-Dispersive X-Ray Spectroscopy.

EtOH: Ethanol.

EU: Eugenol.

FTIR-ATR: Fourier Transform Infrared - Attenuated Total Reflectance.

H_2O_2: Hydrogen peroxide.

H_2SO_4: Sulfuric acid.

HCl: Hydrochloric acid.

IM: Imidazole.

LBL: Layer-by-layer.

MeOH: Methanol.

MOF: Metal-Organic Framework.

MW: Microwave.

n-$BuNH_2$: n-Butylamine.

OAc: Acetate.

PDMS: Poly(dimethylsiloxane).

RITC: Rhodamine B isothiocyanate.

SAM: Self-Assembled Monolayer.

SEM: Scanning Electron Microscopy.

ST: Solvothermal.

SURMOF: Surface-coordinated Metal-Organic Framework.

THF: Tetrahydrofuran.

TLC: Thin Layer Chromatography.

TPEDA: N-(3-(trimethoxysilyl)propyl)ethylenediamine.

$(t\text{-}BuO)_3B$: Tributylborate.

UV-Vis: Ultraviolet-visible spectroscopy.

XRD: X-Ray Diffraction.

μCP: Micro-contact printing.

APPENDICES

APPENDIX 1: MECHANISMS AND ^{1}H NMR, FTIR-ATR, UV-VIS AND FLUORESCENCE SPECTRA

Figure A1. Aldol reaction mechanism.

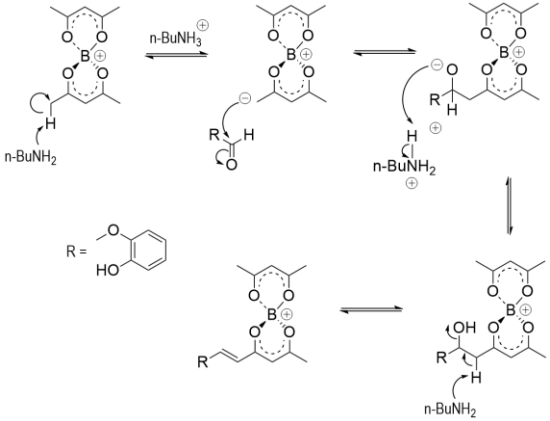

Figure A2: 1H NMR (360 MHz) spectrum of CCM in DMSO-d_6: a) complete spectrum b) area from 8 to 6 ppm.

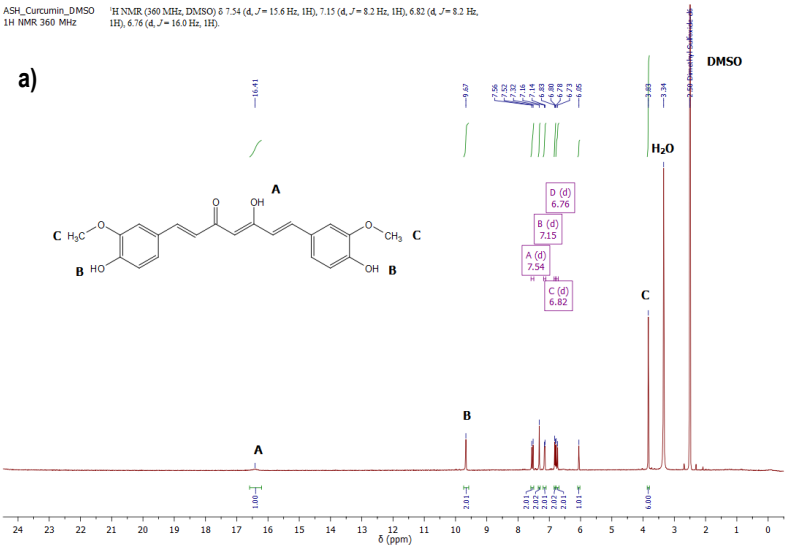

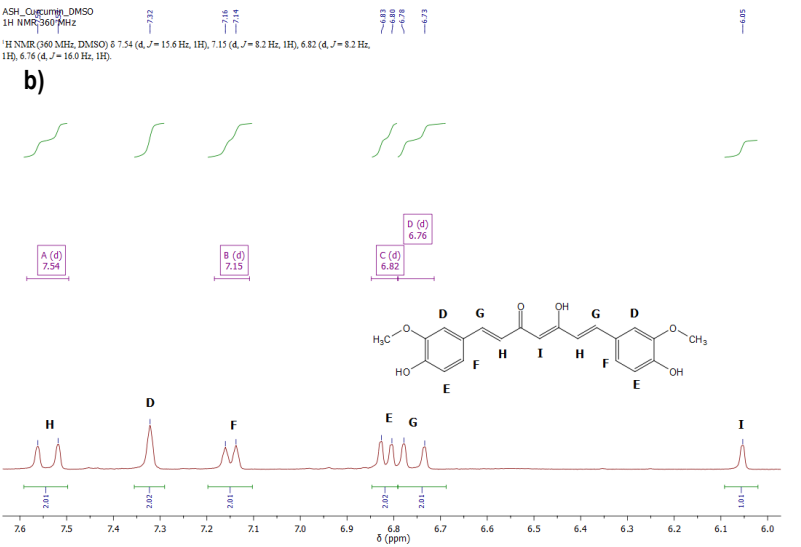

Figure A3. FTIR-ATR spectrum of CCM in solid state (CCM/KBr pellet).

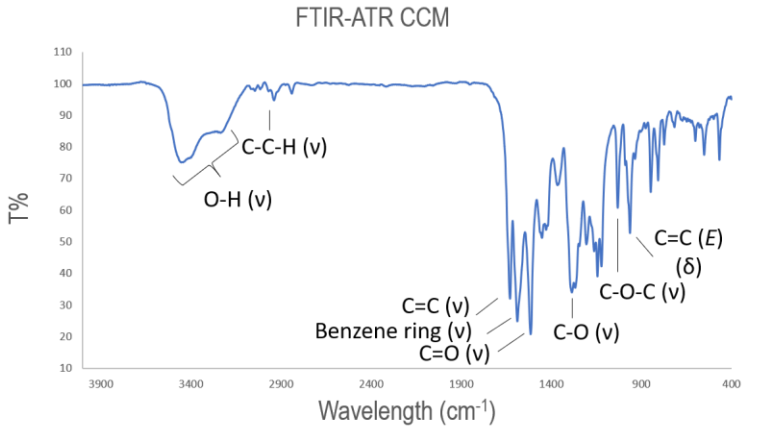

Figure A4. UV-Vis and fluorescence spectra of CCM a) in solid state (fluorescence λ_{exc}: 421 nm, λ_{em}: 573 nm, aperture 10/20) and b) in solution (10^{-5} M in CH_2Cl_2) (fluorescence λ_{exc}: 226 nm, λ_{em}: 497 nm, aperture 5/10; fluorescence λ_{exc}: 420 nm, λ_{em}: 483 nm, aperture 5/5).

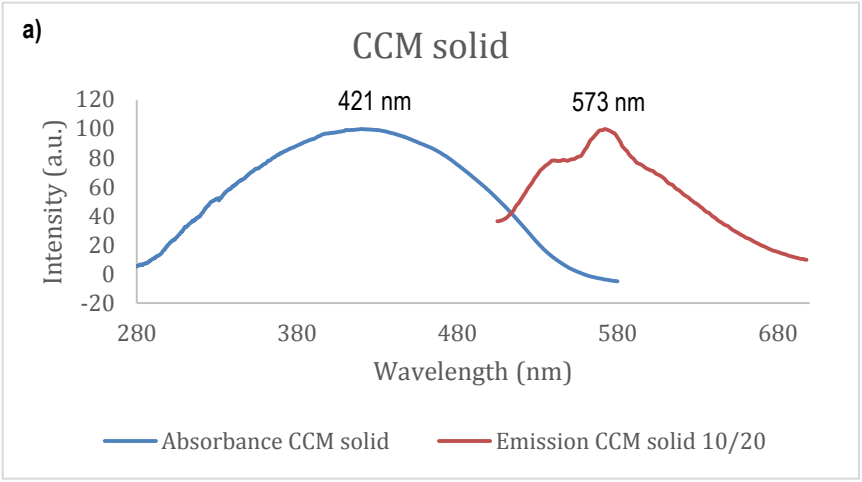

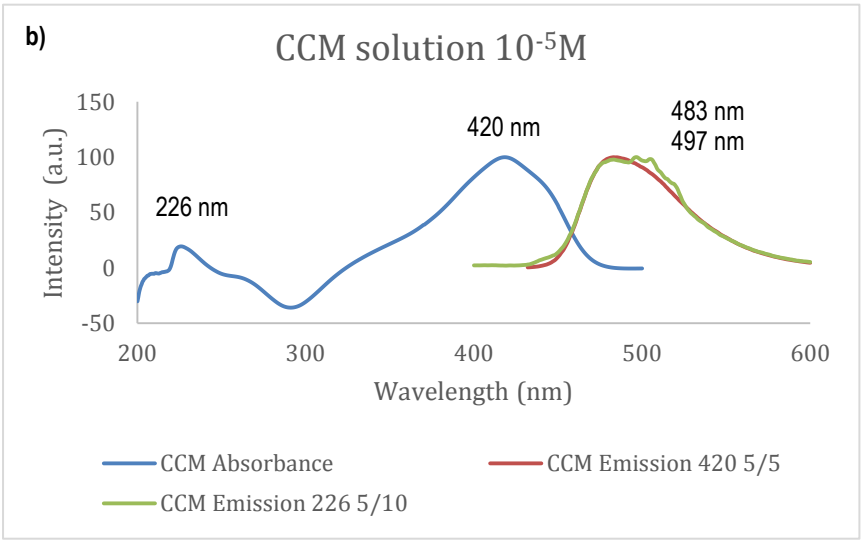

Figure A5. ^{1}H NMR (360 MHz) spectrum of $EUSI(OEt)_3$ in $CDCl_3$ after 30 minutes of reaction (* peaks corresponding to the impurities).

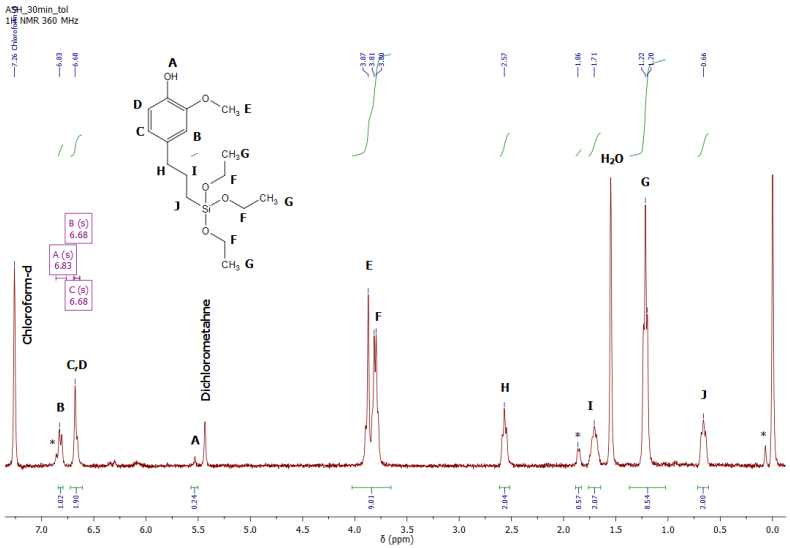

Figure A6. FTIR-ATR spectrum of $EUSi(OEt)_3$.

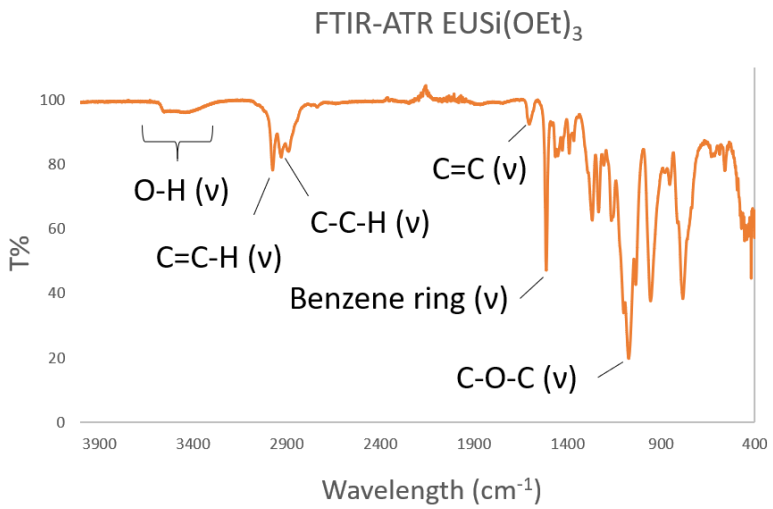

Figure A7. UV-Vis and fluorescence spectra of $EUSi(OEt)_3$ 10^{-5} M solution (fluorescence λ_{exc}: 276 nm, λ_{em}: 320 nm, aperture 5/10).

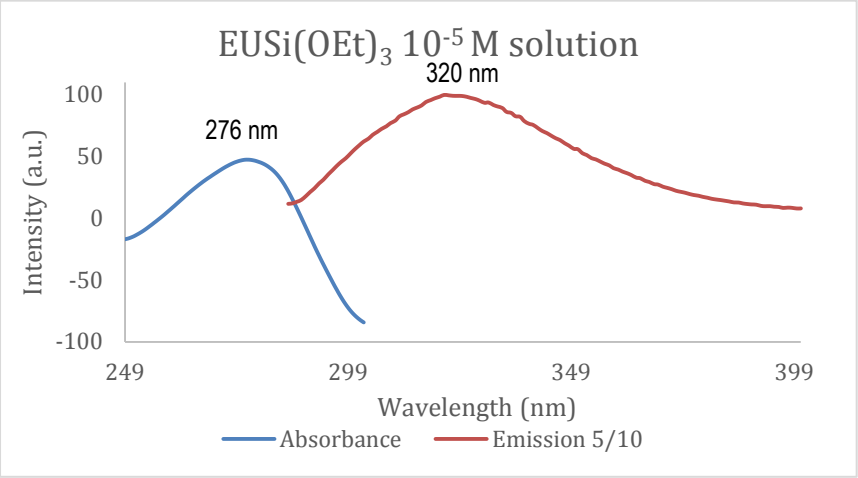

APPENDIX 2: CONTACT ANGLE MEASUREMENTS, EDX AND XPS SPECTRA.

Figure B1. EDX spectra of samples a) **7** (flower **a**, block **b**) and b) **8** (needle **c**, layered spheres **d**).

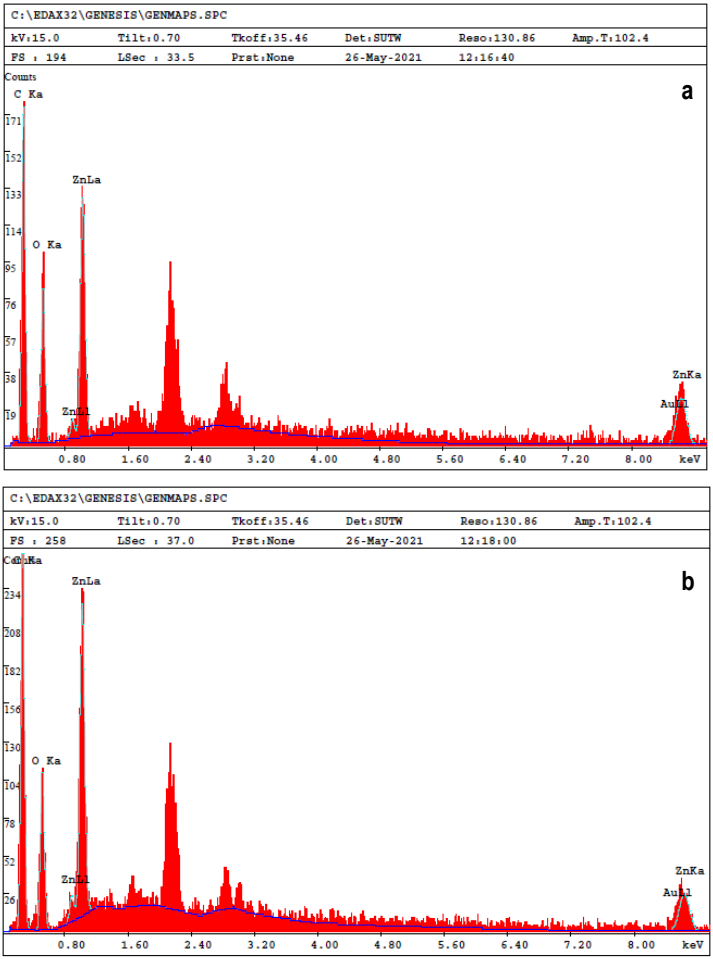

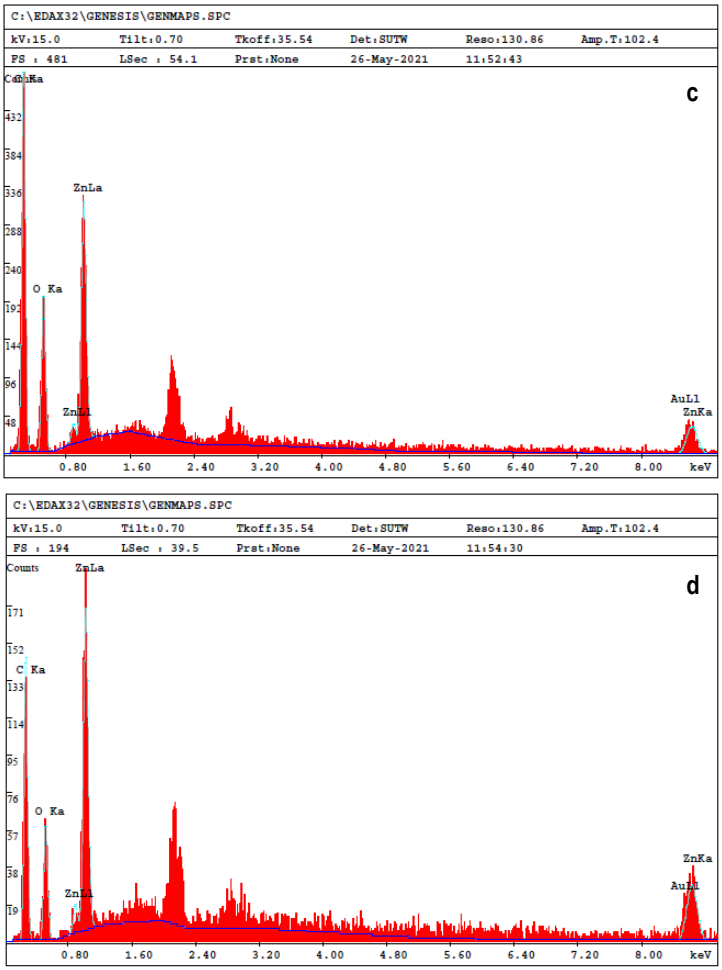

Table B1. Theoretical advancing (Θ_A) and receding (Θ_R) contact angles from NH_2 SAM and IM SAM.[38]

Surface	Θ_A (°)	Θ_R (°)
NH_2 SAM	68 ± 2	55 ± 2
IM SAM	52 ± 2	27 ± 1

Figure B2. XPS spectra of a) NH_2 SAM C1s, b) IM SAM C1s, c) IM SAM N1s and d) CCM N1s.

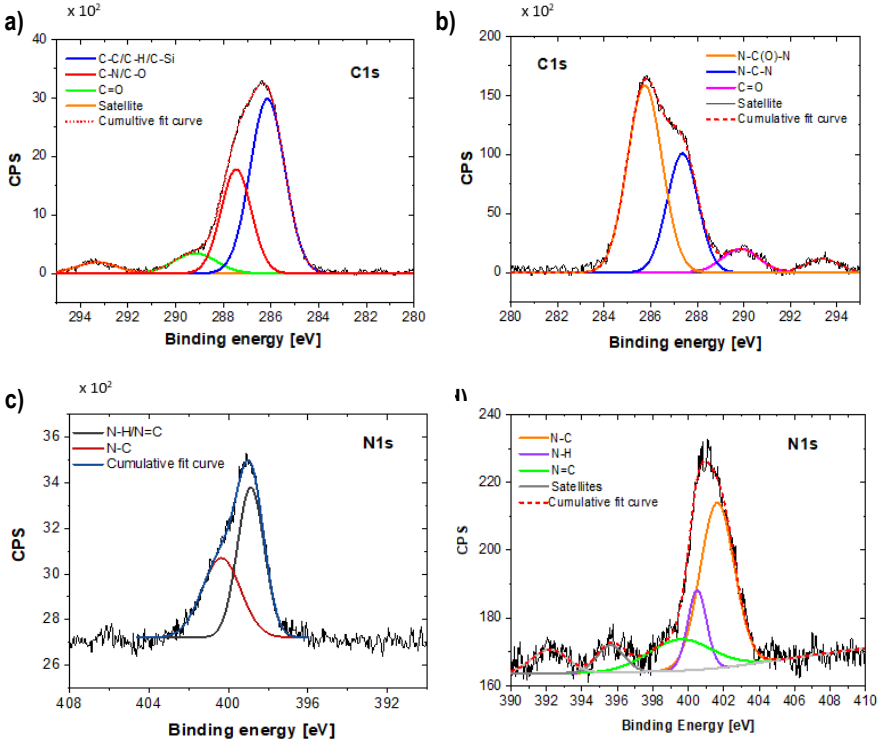

Figure B3. Patterned CCM substrate obtained after a) 4 hours and b) 24 hours immersion in saturated CDI solution and performing µCP. CCM substrates with c) one spot of 5 x 10 µm pattern and d) 10 x 20 µm pattern (Scale bar 30 µm, aperture 8, ImageJ software).

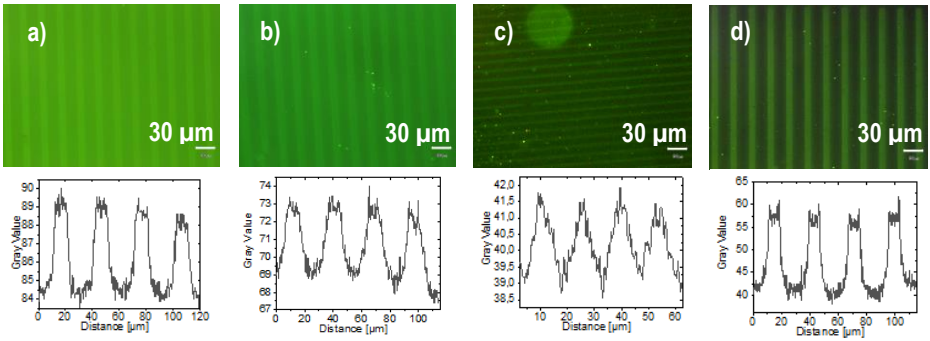

Figure B4. XPS spectra of a) Zn2p CCMZn SAM, b) C1s EU SAM, c) Zn2p EUZn and d) C1s EUZnCCM patterned substrates.

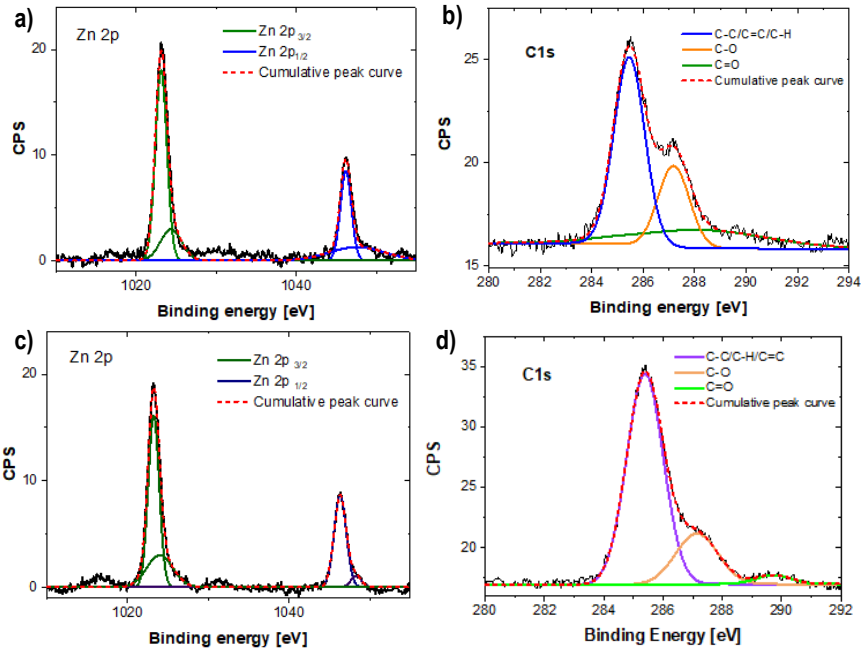

Figure B5. EDX spectrum of the crystal pattern obtained from drop casting technique after backfilling with isopropanol and 1 mM 1-bromo-2,2-dimethylpropane in water.